

AD-A152 283

CRITERIA FOR THE CLASSIFICATION OF HYDROGRAPHIC
POSITIONING DATA(U) NAVAL POSTGRADUATE SCHOOL MONTEREY
CA N E PERUGINI SEP 84

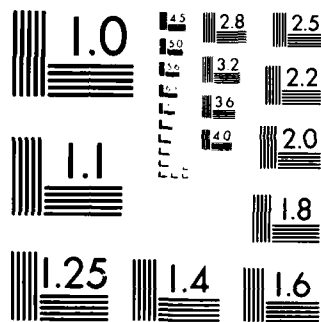
1/1

UNCLASSIFIED

F/G 1777

NL

The table consists of 10 columns and 10 rows. The top row contains 10 black redaction boxes. The remaining 9 rows each contain 10 black redaction boxes, completely obscuring the content of the grid.



MICROCOPY RESOLUTION TEST CHART
NATIONAL BUREAU OF STANDARDS-1963-A

2

AD-A152 283

NAVAL POSTGRADUATE SCHOOL

Monterey, California



DTIC
ELECTE
APR 11 1985
S B D

THESIS

CRITERIA FOR THE CLASSIFICATION
OF HYDROGRAPHIC POSITIONING DATA

by

Nicholas E. Perugini

September 1984

Thesis Advisor:

J. J. von Schwind

Approved for public release, distribution unlimited

DTIC FILE COPY

85. 03 22 073

REPORT DOCUMENTATION PAGE		READ INSTRUCTIONS BEFORE COMPLETING FORM	
1. REPORT NUMBER	2. GOVT ACCESSION NO. ADA152	3. RECIPIENT'S CATALOG NUMBER 253	
4. TITLE (and Subtitle) Criteria for the Classification of Hydrographic Positioning Data		5. TYPE OF REPORT & PERIOD COVERED Master's Thesis September 1984	
		6. PERFORMING ORG. REPORT NUMBER	
7. AUTHOR(s) Nicholas E. Perugini		8. CONTRACT OR GRANT NUMBER(s)	
9. PERFORMING ORGANIZATION NAME AND ADDRESS Naval Postgraduate School Monterey, California 93943		10. PROGRAM ELEMENT, PROJECT, TASK AREA & WORK UNIT NUMBERS	
11. CONTROLLING OFFICE NAME AND ADDRESS Naval Postgraduate School Monterey, California 93943		12. REPORT DATE September 1984	
		13. NUMBER OF PAGES 95	
14. MONITORING AGENCY NAME & ADDRESS (if different from Controlling Office)		15. SECURITY CLASS. (of this report) Unclassified	
		15a. DECLASSIFICATION/DOWNGRADING SCHEDULE	
16. DISTRIBUTION STATEMENT (of this Report) Approved for public release; distribution unlimited			
17. DISTRIBUTION STATEMENT (of the abstract entered in Block 20, if different from Report)			
18. SUPPLEMENTARY NOTES			
19. KEY WORDS (Continue on reverse side if necessary and identify by block number) hydrography, hydrographic surveying, confidence ellipse, confidence circle repeatability, hydrographic positioning			
20. ABSTRACT (Continue on reverse side if necessary and identify by block number) Two methods for evaluating the accuracy of hydrographic positioning data are presented. One method consists of classifying each position in a survey based on the radius of the 90 percent confidence circle. The second method involves classification of positions based on the parameters of the 90 percent confidence ellipse. Both methods are based on geometric and statistical relationships between intersecting lines of position.			

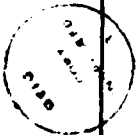
UNCLASSIFIED

SECURITY CLASSIFICATION OF THIS PAGE (When Data Entered)

Range-range, azimuth-azimuth, and range-azimuth positioning data are classified using both criteria. For noncritical positions, the confidence circle method is found to be preferable due to its ease of interpretation. For positions of significant features, such as underwater hazards; the confidence ellipse provides a more useful representation of the shape and orientation of the true error distribution.

The concept of presurvey positioning design is also presented. With the aid of computer graphic displays, the hydrographer can predict the accuracy of offshore positioning data prior to data acquisition. By analyzing accuracy lobes generated about shore stations, a survey can be designed to meet given specifications.

Accession For	
NAVY	<input checked="" type="checkbox"/>
NAVY	<input type="checkbox"/>
NAVY	<input type="checkbox"/>
Distribution/	
Availability Codes	
Dist	Avail and/or Special
A-1	



S/N 0102-LF-014-6601

UNCLASSIFIED

Approved for public release; distribution unlimited.

Criteria for the Classification
of Hydrographic Positioning Data

by

Nicholas E. Perugini
Lieutenant, National Oceanic and Atmospheric Administration
B.S., Pennsylvania State University, 1976

Submitted in partial fulfillment of the
requirements for the degree of

MASTER OF SCIENCE IN HYDROGRAPHIC SCIENCES

from the

NAVAL POSTGRADUATE SCHOOL
September 1984

Author:

Nicholas E. Perugini

Nicholas E. Perugini

Approved by:

Joseph J. von Schwind

Joseph J. von Schwind, Thesis Advisor

Glen R. Schaefer

Glen R. Schaefer, Second Reader

Christopher N. K. Mooers

Christopher N. K. Mooers, Chairman,
Department of Oceanography

John N. Dyer

John N. Dyer,
Dean of Science and Engineering

ABSTRACT

Two methods for evaluating the accuracy of hydrographic positioning data are presented. One method consists of classifying each position in a survey based on the radius of the 90 percent confidence circle. The second method involves classification of positions based on the parameters of the 90 percent confidence ellipse. Both methods are based on geometric and statistical relationships between intersecting lines of position.

Range-range, azimuth-azimuth, and range-azimuth positioning data are classified using both criteria. For noncritical positions, the confidence circle method is found to be preferable due to its ease of interpretation. For positions of significant features, such as underwater hazards, the confidence ellipse provides a more useful representation of the shape and orientation of the true error distribution.

The concept of presurvey positioning design is also presented. With the aid of computer graphic displays, the hydrographer can predict the accuracy of offshore positioning data prior to data acquisition. By analyzing accuracy lobes generated about shore stations, a survey can be designed to meet given specifications.

TABLE OF CONTENTS

I.	INTRODUCTION	9
	A. BACKGROUND	9
	B. ACCURACY STANDARDS FOR HYDROGRAPHIC POSITIONING	11
	C. OBJECTIVES	12
II.	NATURE OF THE PROBLEM	14
	A. HYDROGRAPHIC POSITIONING GEOMETRIES	14
	1. Range-Range	14
	2. Hyperbolic-Hyperbolic	17
	3. Range-Azimuth	19
	4. Azimuth-Azimuth	20
	E. CLASSES OF ERRORS	21
	1. Blunders	21
	2. Systematic Errors	24
	3. Random Errors	27
	C. TREATMENT OF RANDOM ERRORS.	28
	1. One-Dimensional Errors	28
	2. Two-Dimensional Errors	30
	3. Circular Precision Indexes	38
III.	EXPERIMENT DESIGN AND IMPLEMENTATION	49
	A. DATA ACQUISITION PROCEDURES	49
IV.	RESULTS AND DATA ANALYSIS	52
	A. DATA PROCESSING	52
	B. ACCURACY ANALYSIS OF HYDROGRAPHIC POSITIONING DATA	53
	C. ACCURACY PREDICTIONS	59

V.	CONCLUSIONS AND RECOMMENDATIONS	67
A.	ACCURACY SPECIFICATIONS	67
B.	USES FOR ACCURACY FIGURES	71
APPENDIX A:	SUBROUTINE FOR 90 PERCENT CONFIDENCE	
	CIRCLE PARAMETERS	74
APPENDIX B:	ACCURACY CLASSIFICATION: 90 PERCENT	
	CONFIDENCE CIRCLES	76
APPENDIX C:	PROGRAM FOR 90 PERCENT CONFIDENCE	
	ELLIPSE PARAMETERS	85
APPENDIX D:	ACCURACY CLASSIFICATION: 90 PERCENT	
	CONFIDENCE ELLIPSES	88
LIST OF REFERENCES	91
INITIAL DISTRIBUTION LIST	93

LIST OF TABLES

I.	Values of the Constant K	34
II.	Probabilities Associated With d_{rms}	42
III.	Probabilities, Given c and R	44
IV.	Radii of Circles Given c and P	45
V.	Coordinates of Control Stations	53
VI.	Linear Approximations for K as a Function of c	55
VII.	β Limits for Surveys	68
VIII.	Accuracy Figures for $\sigma_1 = \sigma_2 = 1.3 \text{ m}, \rho_{12} = 0$	69
IX.	Accuracy Figures for $\sigma_1 = \sigma_2 = 3 \text{ m}, \rho_{12} = 0$	70
X.	Accuracy Figures for $\sigma_1 = \sigma_2 = 10 \text{ m}, \rho_{12} = 0$	70

LIST OF FIGURES

2.1	Geometry of a Range-Range Position	17
2.2	Geometry of a Hyperbolic-Hyperbolic Position . .	19
2.3	Geometry of an Azimuth-Azimuth Position	22
2.4	The Normal Distribution	29
2.5	Circular Normal Distribution	32
2.6	Error Ellipse Formed by Two Uncorrelated LOP's	33
2.7	Coordinate Transformations for Correlated LOP's	36
2.8	Error Ellipses Around a Range-Range System . . .	39
2.9	The d_{rms} Error Circle	41
3.1	Hydrographic Survey Area	50
4.1	Range-Range Accuracy Analysis	56
4.2	Azimuth-Azimuth Accuracy Analysis	57
4.3	Construction of a Reliability Curve	61
4.4	Reliability Contours: Range-Range Geometry . .	63
4.5	Reliability Contours: Azimuth-Azimuth Geometry	64
4.6	Range-Range Point Accuracy Prediction	65
4.7	Azimuth-Azimuth Point Accuracy Prediction . . .	66

I. INTRODUCTION

A. BACKGROUND

A hydrographic record can be viewed as the resultant of two independent measurements made at a discrete point over a body of water. These measurements involve the determination of a vessel's position at a given time as well as the depth of water at that position. Of interest to the hydrographer and to the user of hydrographic data is the accuracy of the position determinations. Fundamental to the determination of positional accuracy is the identification of the sources of errors in position measurements and the ultimate treatment of these errors.

A hydrographic position can be determined by a number of methods all involving geometric relationships between known points and the vessel's unknown location. The known points may be fixed stations on shore, whose coordinates have been determined by geodetic survey methods, or they may be rapidly moving satellites whose coordinates in time and space can be defined very precisely. A hydrographic position is established by the intersection of two or more lines of position (LOP's) which are generated by the geometric relationships between the fixed points and the vessel's unknown location. The resultant accuracy of the vessel's position is therefore, in part, a function of the errors associated with the intersecting LOP's.

Several measures of accuracy can be used to evaluate the quality of a hydrographic position. Predictability, or absolute accuracy, is the measure of accuracy with which the positioning system can define the location of the same point in terms of geographic coordinates. Repeatability, or

relative accuracy, is a measure with which a positioning system permits a user to return to a specific point on the earth's surface in terms of the LOP's generated by the system [Ref. 1, p. 14]. With the elimination of all systematic or bias errors, the terms repeatability and predictability become identical. Hydrographic surveyors usually work toward this condition, although it is not always achievable.

Heinzen [Ref. 2] and Burt [Ref. 3] have presented several techniques for quantifying the repeatable accuracy for offshore positions. These techniques have roots in the statistical treatment of random error. Although the methods have been well documented, no single criterion to classify the accuracy of a hydrographic position has been agreed upon by the international hydrographic community.

Preceding the development of automation in hydrograph data acquisition and processing, the task of calculating an accuracy figure to attach to each position in a hydrographic survey was unthinkable. To ensure overall accuracy in a survey, certain generalizations were developed to act as guidelines. For example, the U.S. Coast and Geodetic Survey Hydrographic Manual [Ref. 4, p. 217] states the following concerning the strength of a three-point fix:

The fix is strong when the sum of the two angles is equal to or greater than 180° and neither angle is less than 30° . The nearer the angles equal each other the stronger will be the fix.

Generalizations of this type provided useful qualitative guidance for assuring a degree of positional accuracy and many are still in existence today.

With the aid of computers, the hydrographer now has the capacity to evaluate the accuracy of positioning data for an entire survey. An accuracy figure can be computed for each position in a survey and stored in a data base along with

other survey information. This figure may provide useful information for users of the data, as well as a yardstick for the hydrographer to evaluate the quality of the work. Furthermore, a presurvey accuracy analysis enables a survey to be designed to meet desired specifications.

E. ACCURACY STANDARDS FOR HYDROGRAPHIC POSITIONING

In 1982, the International Hydrographic Organization (IHO) published new recommendations for error standards concerning the accuracy of hydrographic positions. These standards [Ref. 5] are:

The position of soundings, dangers and all other significant features should be determined with an accuracy such that any probable error, measured relative to shore control, shall seldom exceed twice the minimum plottable error at the scale of the survey (normally 1.0 mm on paper). It is most desirable that whenever positions are determined by the intersection of lines of position, three such lines be used. The angle between any pair should not be less than 30°.

Most statisticians define the term "probable error" as that error occurring at the 50 percent probability level. However, the author of the IHO standards, Commodore A.H. Cooper RAN (Ret.) has stated that the term "probable error" was intended to have no statistical significance. Munson interpreted the words "shall seldom exceed" to mean 10 percent of the time [Ref. 6]. Using this interpretation, the first sentence of the specification might be written:

The position of soundings, dangers and all other significant features should be determined with an accuracy such that any error in position measured relative to shore control will fall within a circle with radius of the minimum plottable error at the scale of the survey (normally 1.0 mm. on paper), with 90 percent confidence.

The specification in this form could be evaluated quantitatively. The criterion for defining accuracy in terms of a fixed probability is common in the field of surveying. For example, the standards of accuracy developed for geodetic

These errors are usually small in magnitude and can be eliminated by proper adjustment of the instrument by either the manufacturer or a qualified technician.

The field hydrographer has ultimate control over the geometric systematic errors associated with a theodolite. In range-azimuth positioning the theodolite and transmitter may occupy the same horizontal control station. If the theodolite is not set directly over the station a resultant systematic error will occur in all measurements. It can be shown that these errors are non-linear but do follow a mathematical relationship. Likewise, if the transmitter is not located directly over the station, a similar type of bias occurs. Depending on the eccentricity of the theodolite, the vessel's range from the theodolite, and the scale of the survey--these errors can seriously affect the absolute accuracy of the offshore positions.

In a similar fashion, it is also imperative to position the target directly over the horizontal control station used as an initial. Failure to do this will result in an error which will be propagated to offshore positions.

Many situations arise in the field where it is advantageous to set a transmitter and theodolite over a single horizontal control station. Frequently it is feasible to construct a platform to accommodate both instruments; in a case where it is not, the position of an eccentric horizontal control station near the original station should be determined and that station used for the location of one of the instruments. The theodolite and the transmitter then occupy two known stations and the geometric source of systematic error is eliminated.

b. Electronic Ranging Systems

The systematic errors associated with electronic positioning systems are complex in nature and functions of

2. Systematic Errors

Systematic errors occur with the same sign, usually of similar magnitude, and can be expressed in terms of a mathematical model. Systematic errors follow a defined pattern and occur in a number of consecutive related observations. Repetition of measurements does nothing to minimize their effect. In the case of hydrographic positioning, systematic errors are identified and modeled by calibration of the measuring instrument against a known standard. The following is a brief discussion concerning systematic errors and their treatment in relation to hydrographic positioning equipment.

a. Theodolites

In nearshore surveys the theodolite is used primarily for range-azimuth and azimuth-azimuth positioning. Systematic errors associated with the theodolite can be classified into two groups: those associated with the physical design of the instrument and those involving the geometry of the positioning scheme. Some sources of systematic errors [Ref. 8] associated with the physical characteristics of a theodolite are:

- i. The horizontal circle may be eccentric.
- ii. Graduations on the horizontal circle may not be uniform.
- iii. The horizontal axis of the telescope (about which it rotates) may not be perpendicular to the vertical axis of the instrument.
- iv. The longitudinal axis of the telescope may not be normal to the horizontal axis.
- v. The telescope axis and the axis of the leveling bubble may not be parallel.

range-azimuth fix. A range and an azimuth are generated from a known control station to the vessel's position. A second control station is used to fix the initial azimuth; a third shore control station is located 10 meters from the initial station and its coordinates are mistakenly used for the initial station in plotting. The resultant hydrographic position is in error, but this error will not be easily distinguished.

Although most blunders have their origin in human carelessness, some can be attributed to equipment malfunction. For example, microwave systems which generate IOP's are known to become unsteady under certain conditions. Spurious range readings resulting from signal reflections can be recorded as true positioning data. In this case, the blunder may or may not be easily detected.

In automated data acquisition systems, software has been developed to detect the occurrence of anomalous range readings. By inputting a course and speed of a vessel traveling along a line, the computer can determine if the recorded position is valid based on the principle of dead reckoning. If the recorded position is found to be invalid the hydrographer will be immediately alerted to the situation and can take action to remedy the problem. In non-automated systems the principle of dead reckoning is applied manually. Given the course and speed of the vessel, the validity of the position can be checked with spacing dividers. This involves checking the spacing between fixes recorded before and after the position in question.

Before any type of error analysis is to be performed on the hydrographic positioning data, it is essential that all blunders be identified and properly treated. In general, careful planning coupled with thorough checking will minimize the occurrence of blunders.

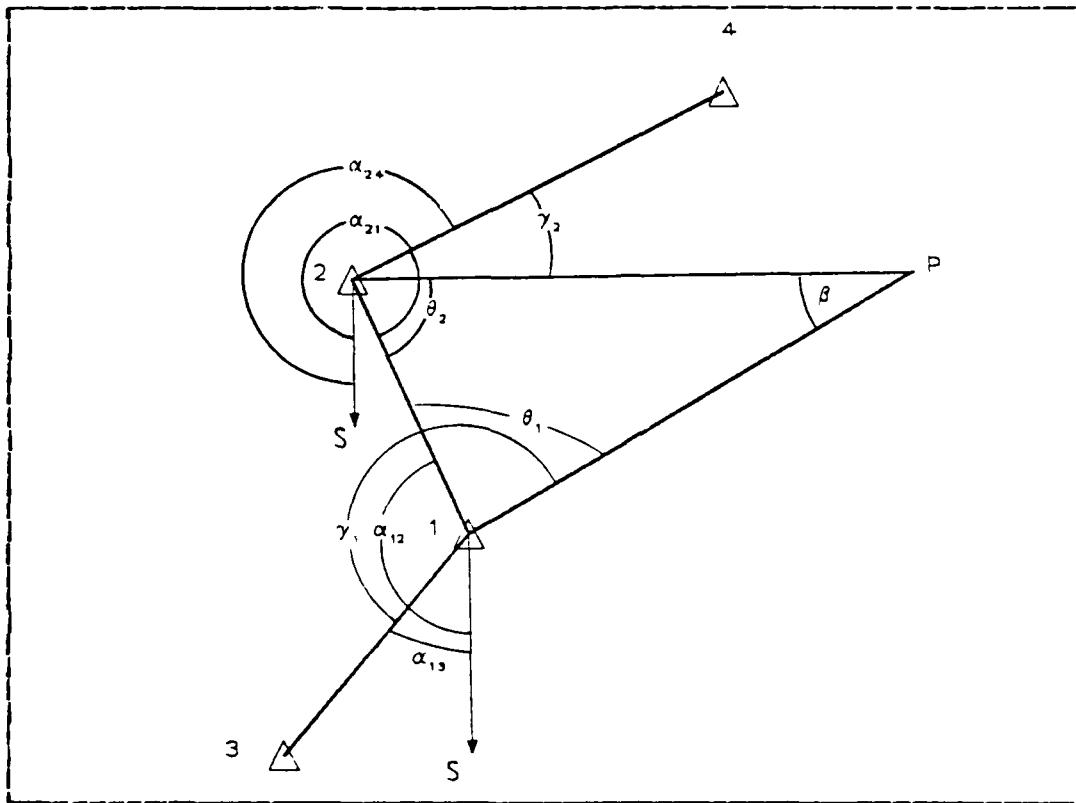


Figure 2.3 Geometry of an Azimuth-Azimuth Position

Consider the following as an example of a blunder associated with range-range geometry. An offshore position is to be determined by the intersection of two electronic IOP's generated from transmitters located on known shore stations. The vessel is working west of a shoreline that runs generally in a north-south direction. As the hydrographer faces the stations from sea, the southern shore station is mistakenly identified as left and the northern shore station as right. The resultant offshore position will plot to the east of the base line. This blunder is readily detected and can be easily remedied.

Not all types of blunders are so easily detected. Suppose an offshore position is to be determined by a

occupy stations 1 and 2, and initial on stations 3 and 4, respectively, the observer at station 1 measures angle γ_1 and the observer at station 2 measures γ_2 to the vessel. The angle of intersection, β , is then computed by first determining the forward azimuths, measured clockwise from the south, from stations 1 to 2 (α_{12}), 1 to 3 (α_{13}), 2 to 1 (α_{21}), and 2 to 4 (α_{24}). The interior angles, θ_1 and θ_2 , of triangle 12P are

$$\theta_1 = |\alpha_{13} + \gamma_1 - \alpha_{12}| \quad (2.8)$$

and

$$\theta_2 = |\alpha_{24} + \gamma_2 - \alpha_{21}| \quad (2.9)$$

so the angle of intersection, β , at the vessel's location is

$$\beta = 180^\circ - (\theta_1 + \theta_2) \quad (2.10)$$

E. CLASSES OF ERRORS

All hydrographic positioning measurements are subject to error. The following sections discuss categories of errors and methods used to treat these errors.

1. Blunders

Blunders are gross mistakes which are generally due to the carelessness of the observer. Blunders can vary in magnitude, ranging from large errors which are easily detected, to small errors which may be barely distinguished. They can be detected by making repeated observations or by carefully checking the data in the processing phase. Blunders occur in various forms and most can be avoided by carefully planning the data acquisition process.

in this arrangement but systems employing a laser can also be used for short-range work. Another LOP is generated by fixing an azimuth from a shore control station to the vessel. A second control station is used for an initial azimuth by the observer. Azimuth determinations can be made after observing directions with a theodolite as an observer tracks the moving vessel.

There are two ways to determine a range-azimuth position. The most common way is to have the theodolite and the transmitter occupy the same shore control station. Hence, the angle of intersection, β , of the LOP's is always 90° . This arrangement is commonly used by the National Ocean Service (NOS) for large-scale nearshore surveys.

The other way is to have the theodolite and the transmitter occupy two different control points. Then the geometry is similar to that of the range-range position. The angle of intersection, β , is computed by trigonometric relationships among the azimuth of a line between the shore stations, the observed direction to the vessel, and the measured range to the vessel.

4. Azimuth-Azimuth

Azimuth-azimuth positioning geometry is used for nearshore high-accuracy surveying. Theodolites are set over two control stations on shore. The vessel is sighted on simultaneously by the two theodolite observers, generating two visual LOP's whose intersection define the vessel's location. Initial azimuths are fixed by sighting on control stations which are visible to the observers.

The angle of intersection for an azimuth-azimuth position is dependent on the geometric relationships between the occupied stations, the initial stations, and vessel's position (Fig. 2.3). Assuming that theodolite observers

where the term $1/\sin(\alpha/2)$ is called the lane expansion factor. The angle of intersection, β , between the two hyperbolas is then given by

$$\beta = \frac{\alpha_r + \alpha_g}{2} \quad (2.7)$$

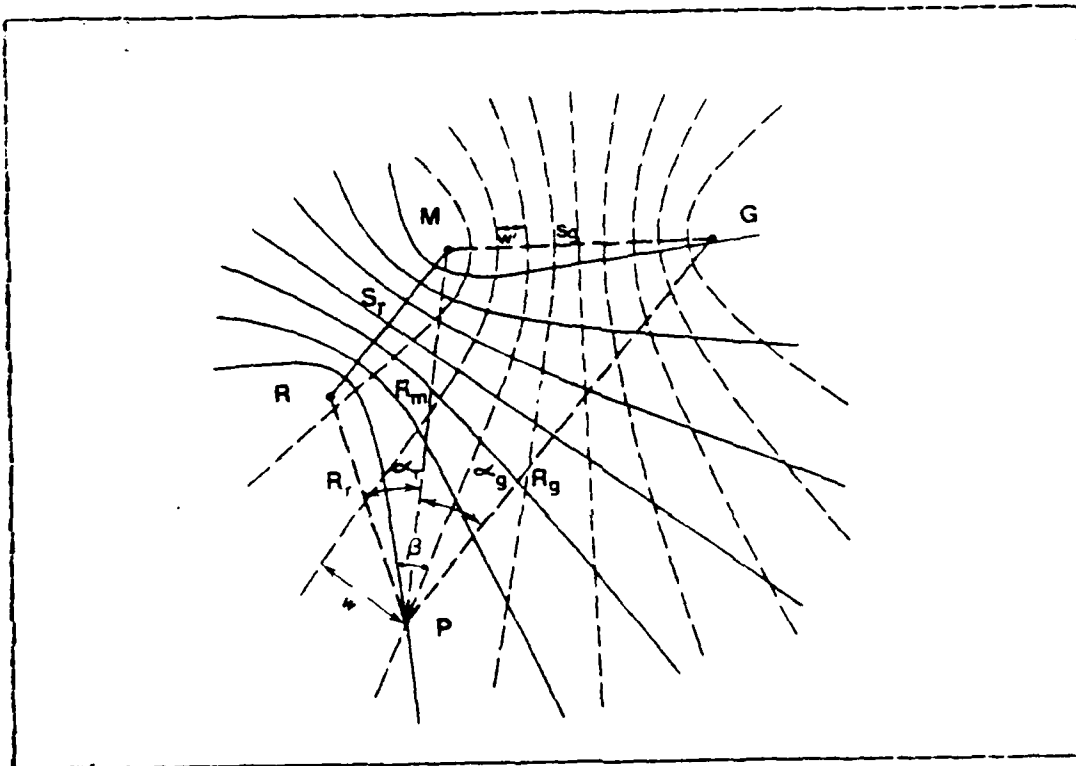


Figure 2.2 Geometry of a Hyperbolic-Hyperbolic Position

3. Range-Azimuth

This positioning geometry is used for nearshore, line-of-sight surveys. One LOF is generated by an electronic range originating from a transmitter located on a shore control station. A microwave system is commonly used

Hyperbolic location methods can be divided into two groups based on the electronic principles used to define the distance differences [Ref. 7, p. 87]. Loran is an example of a pulse system in which the differences in times of arrival of pulses transmitted by the master-slave combinations are translated into distance differences. The resultant position has no lane ambiguity and is easily resolved. The second method of hyperbolic positioning involves measuring a phase difference from two master-slave combinations at the vessel's position. The phase difference translates into a fractional lane count which in itself provides an ambiguous position. This ambiguity is resolved by using a whole-lane counter which is initialized at a known geographical point. In hyperbolic positioning, the ship is in a passive mode and the system can be used by many vessels.

The angle of intersection between the two hyperbolas can be computed by first defining the following quantities:

- S_r is the length of red base line,
- S_g is the length of green base line,
- R_m is the distance between master and vessel's position P,
- R_r is the distance from red slave to point P,
- R_g is the distance from green slave to point P,
- α_r is the angle between lines PM and PR, and
- α_g is the angle between lines PM and PG.

The spacing between lanes increases with distance from the master-slave pair. The lane widths along the base line are

$$w'_r = \frac{\lambda_r}{2} \quad \text{and} \quad w'_g = \frac{\lambda_g}{2} \quad (2.5)$$

Then the lane widths at any point P are

$$w_r = \frac{\lambda_r}{2} \left(\frac{1}{\sin(\alpha_r/2)} \right) \quad \text{and} \quad w_g = \frac{\lambda_g}{2} \left(\frac{1}{\sin(\alpha_g/2)} \right) \quad (2.6)$$

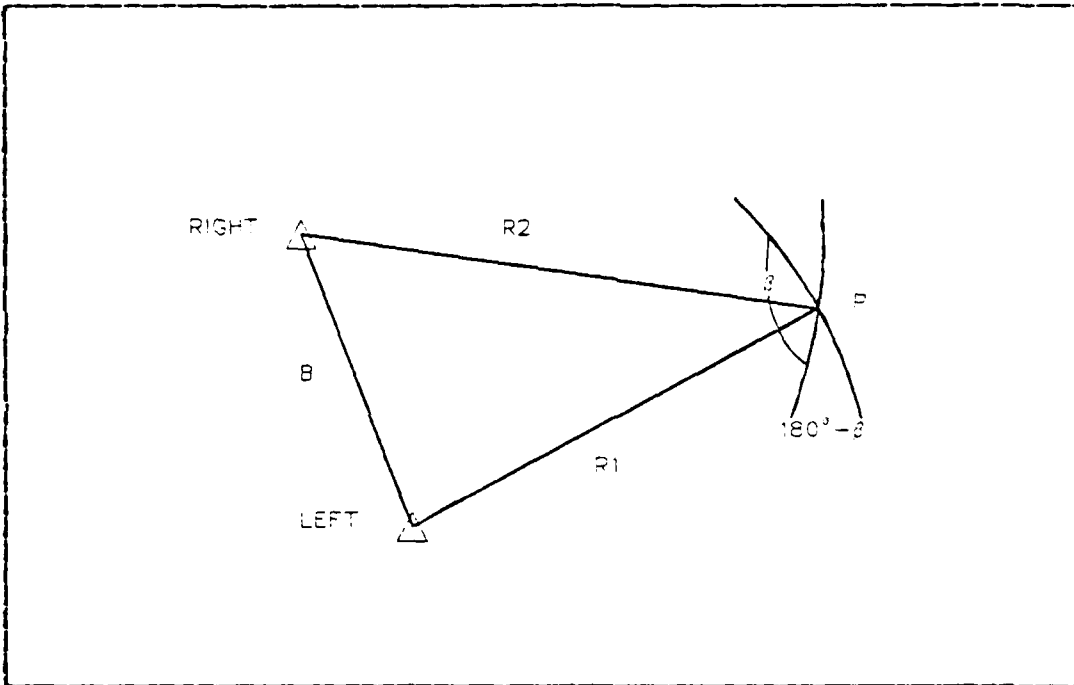


Figure 2.1 Geometry of a Range-Range Position

2. Hyperbolic-Hyperbolic

Hydrographic positioning by hyperbolic-hyperbolic geometry utilizes the intersection of two hyperbolas each generated about a pair of shore control stations. A hyperbola is the locus of points in which the difference of distance from two fixed points is always constant. A three-station hyperbolic net is the most commonly used hyperbolic mode for offshore survey (Fig. 2.2). One family of hyperbolas (Red) are generated about a master station, M, and a slave, R; while a second family of hyperbolas (Green) are generated with respect to the master and a second slave, G. For the first family of hyperbolas, the control points M and R act as the foci, while points M and G act as the foci for the second family.

problem of lane ambiguity must be addressed. Ranges are expressed in full and partial lane counts where a lane width w is

$$w = \frac{\lambda}{2} \quad (2.2)$$

where λ is the wavelength of the transmitting frequency, f , and given by

$$\lambda = \frac{c}{f} \quad (2.3)$$

Medium-range systems commonly in use today are Cubic Western's "ARGO," Hasting Raydist's "Raydist," and Odom Offshore's "Hydrotrack."

The angle of intersection associated with a range-range position is computed from a simple trigonometric relationship. The vessel's position P (Fig. 2.1) is determined by the intersection of the ranges from the left and right shore stations, R_1 and R_2 respectively. B is the base line distance computed between the two known shore stations. Since the range circles from the shore stations intersect at two points, it is necessary for the plotter to recognize which side of the base line the vessel is on in order to eliminate the ambiguity. The angle of intersection of the two LOP's (β) is given by the law of cosines

$$\beta = 180^\circ - \text{Arc cos} \left(\frac{B^2 - R_1^2 - R_2^2}{2 R_1 R_2} \right) \quad (2.4)$$

In qualitative terms, the fix is strongest when β approaches 90° . Most hydrographic specifications limit the angle of intersection from a minimum of 30° to a maximum of 150° .

An electronic positioning system may be active or passive. In an active system, a transmitter from the survey launch keys the transmission of ranges from the shore station. In turn, the signals generated from the shore stations (slaves) are then received by the launch. An active system is limited to a finite number of users, usually not more than about four. The number of users of a passive system is unlimited as the survey launch requires only a receiver which is constantly listening for signals which are being transmitted from shore.

Short-range, or line-of-sight, positioning systems are used for nearshore hydrographic surveys. These systems operate in the microwave region of the electromagnetic spectrum (3 to 10 GHz). A distance is determined by observing the time needed for a pulse to travel from a master transponder located aboard the survey vessel to a remote transponder on shore and back to the master transponder. Knowing the average velocity of the electromagnetic pulse, the distance D is then

$$D = \frac{c t}{2} \quad (2.1)$$

where c is the group velocity of the wave packet and t is the two-way travel time. Short-range systems which are in wide use today are Racal Decca's "Trisponder" and Motorola's "Mini-Ranger." These systems have direct range readout and are readily interfaced into a navigational computer and a data acquisition system. Both systems are active and user limited.

Medium-range positioning systems operate in the 1- to 5-MHz frequency range of the electromagnetic spectrum. A distance is determined by measuring the phase relationship between transmitted and received waves. These systems are usually referred to as continuous wave systems and the

II. NATURE OF THE PROBLEM

The development of an accuracy figure for offshore positions is inherently tied to the geometry of the positioning method and the errors which are associated with the positioning equipment that is used. This chapter will discuss the geometric and statistical elements involved in determining an offshore position and presents several methods for quantifying repeatable accuracy.

A. HYDROGRAPHIC POSITIONING GEOMETRIES

An offshore fix can be determined by the intersection of two or more LOP's. These LOP's may be generated by electronic or visual means. Working toward the development of an accuracy index, it will be necessary to compute the angle of intersection of the LOP's associated with different positioning geometries. The following sections discuss the geometry of conventional offshore positioning methods and ways to compute the angles of intersection. This thesis will not address the geometry involved in a three-point sextant fix.

1. Range-Range

Establishing an offshore fix by range-range geometry involves measuring distances electronically from fixed positions on shore to the vessel's unknown location. Ranges can be determined by measuring the elapsed time between transmission and receipt of a radio pulse or by comparing the phase of the transmitted wave with the phase of the received wave [Ref. 2]. In each case, transmitters are set on stations on shore whose coordinates are determined by precise land survey methods.

method of classification is a useful index for quantifying the accuracy of positions. The computed radii of the 90 percent confidence circles can serve as an accuracy figure that can be attached to each position in a survey and stored in a data base.

The third objective of this thesis is to demonstrate that a presurvey analysis can be used in designing positional accuracy to meet specifications. The existing general guidelines for planning can be better defined. For example, in planning a survey hydrographers usually lay out circles which delimit the 30° and 150° boundaries that define the minimum and maximum allowable intersection angles between two LOP's. As a means to meet accuracy requirements, it can be shown that these limits should vary based on the scale of the survey and the precision of the positioning equipment.

control surveys have their origin in probability theory. Procedures for obtaining first-order geodetic positions require sixteen repeated theodolite observations of each direction. Lower order positions require fewer numbers of observations. Given the precision of one observation of each direction, it can be demonstrated that increasing the number of observations coincides with increasing the probability of the direction falling within specified limits.

Regarding accuracy determinations, there are several problems unique to hydrographic surveying. Whereas standards for other types of surveys rely on multiple observations of the same quantity, the accuracy of a hydrographic position must be evaluated in terms of a single observation (which may be the intersection of two or more LOP's). Diverse methods for obtaining a hydrographic position exist and these methods must all be evaluated using the same criterion. Also, there is a broad spectrum of equipment used in hydrographic positioning and in many cases the precision of this equipment is not well defined.

C. OBJECTIVES

A need exists to give quantitative meaning to the accuracy specifications set forth by the IHO. One of the objectives of this thesis is to demonstrate that defining the specifications in terms of the fixed 90 percent confidence level is a valid interpretation. By defining what the specifications imply, procedures can be developed to meet the standards.

A second objective of this thesis is to apply the theory of errors, associated with hydrographic positioning, to a data set. This analysis involves classifying positioning data acquired in a survey based on the radii of circles of equivalent probability. It will be demonstrated that this

many variables. Munson [Ref. 9, p. 4] addresses several problems associated with short-range systems used in hydrographic surveys. The most common problems with short-range systems are variation in range and calibration drift with time. Variations in internal equipment time delays in the transmitter, the transponder, or the receiver can induce errors in measured ranges. For pulse systems such variations can occur due to temperature dependence of components and fluctuations in signal strength at the transponder. Multipath effects are also a problem. Under some circumstances a reflected wave and the directly transmitted wave arrive with a phase difference of 180° . Cancellation or fading of the directly transmitted signal can result.

NOS conducts base line calibrations of short-range positioning systems periodically during the course of a survey to minimize or eliminate systematic error. In this process, a transmitter and receiver are each placed over control stations on shore and the measured range is compared to the true range. In this way the systematic error is eliminated by zeroing the instrument or by applying a constant correction to raw data. System checks are performed daily to assure there is no drift from the original calibration. A check can be accomplished by comparing a position defined by the ranging system to a known fixed-point position, to a sextant fix position, or an intersection position.

Munson [Ref. 9, p. 5] also discusses sources of systematic errors associated with medium-range systems. The most significant systematic errors occur as a function of position due to varying propagation velocity. The medium-range electronic signal propagation velocity depends on the surface conductivity and transmission path (over water, over land, or over different types of land). Because of this dependence, systematic errors as a function of position

occur at different effective phase velocities. Knowing the propagation velocity to use, or the phase correction to make as a function of range, is a problem. Sky wave and storm interference also pose problems. At extreme ranges of operation, sky wave interference can affect the more predictable ground wave, especially during nighttime operations. Lane ambiguities are also a problem. Most systems are inherently ambiguous and must be zero set and continually monitored for lane jumps or loss of signal which results in the loss of lane count.

NOS uses several techniques to determine the systematic error associated with medium-range positioning systems. These techniques involve determining a whole and partial lane count for phase comparison systems. Two of the more widely used techniques are comparison of three-point sextant fix positions to positions determined by the electronic ranging system and calibration of the electronic system at a fixed point. In both techniques the whole lane counts are fixed by the calibration; correctors to the partial lane count are determined and applied to the raw ranging data.

3. Random Errors

Random errors are chance errors, unpredictable in magnitude or sign, and are governed by the laws of probability [Ref. 10, p. 1206]. They are errors which remain after blunders and systematic errors have been removed. Random errors result from accidental and unknown combinations of causes and are beyond the control of the observer. Greenwalt [Ref. 12, p. 2] states they are characterized by:

- i. Variation in sign; positive errors occur with equal frequency as negative ones.
- ii. Small errors occur more frequently than large errors.
- iii. Extremely large errors rarely occur.

Random errors are unique to specific types of positioning equipment and vary in magnitude depending on the precision of the instruments that are used. The following section outlines statistical methods for their treatment.

C. TREATMENT OF RANDOM ERRORS.

1. One-Dimensional Errors

Certain basic statistical quantities must first be defined in the analysis of random errors. Consider a vessel moored securely to a fixed offshore platform. A number of ranges, n , from a microwave transmitter located on a shore control station are recorded. The mean of these observations is

$$\mu_x = \frac{\sum_{i=1}^n x_i}{n} \quad (2.11)$$

where x_i represents an individual observation. The standard error, s , of the observations is then

$$s = \sqrt{\frac{1}{n-1} \sum_{i=1}^n (x_i - \mu_x)^2} \quad (2.12)$$

where the quantity $(x_i - \mu_x)$ is referred to as the residual, or true error, v_i , of a particular observation. As n gets very large, the factor $1/n$ can be substituted for $1/(n-1)$ in Equation 2.12. Likewise, in treating the large sample, σ can be substituted for s and μ for μ_x , where μ and σ are the mean and standard error of the entire population.

It is of interest to determine the probability of occurrence of a particular observation. The normal or Gaussian distribution equation relates the residual of a particular random variable with the probability of its

occurrence, and is given by

$$P(v) = \frac{1}{\sigma\sqrt{2\pi}} e^{-\left(\frac{v^2}{2\sigma^2}\right)} \quad (2.13)$$

The plot of this equation yields the normal distribution curve (Fig. 2.4). The height of the curve above the vertical axis is proportional to the probability of a particular error occurring.

The probability of a residual falling between any two residuals v_1 and v_2 can be computed by integrating Equation 2.13 as

$$P(v) = \int_{v_2}^{v_1} \frac{1}{\sigma\sqrt{2\pi}} e^{-\left(\frac{v^2}{2\sigma^2}\right)} dv \quad (2.14)$$

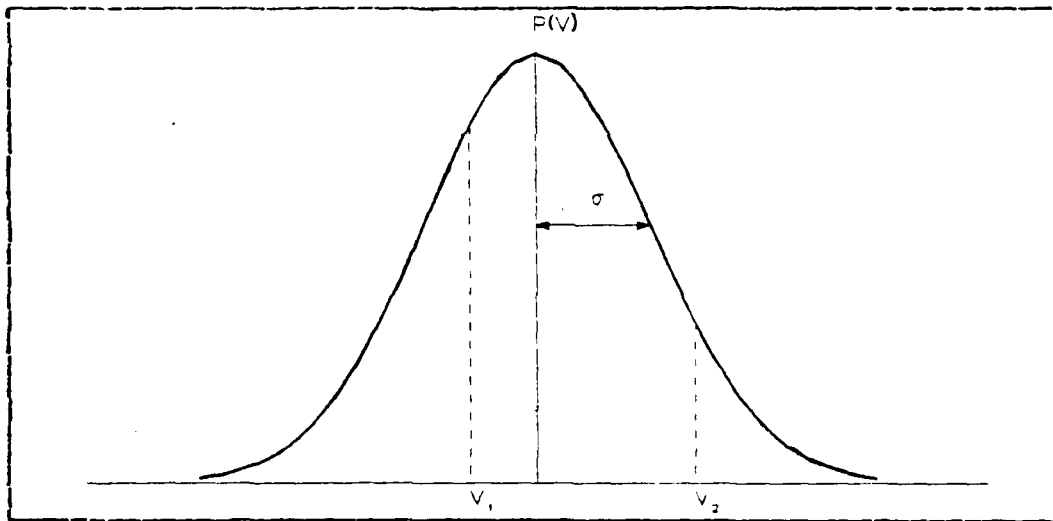


Figure 2.4 The Normal Distribution

This integral is difficult to evaluate analytically so tables have been compiled to aid in computations. For $v_1 = +\sigma$ and $v_2 = -\sigma$, it can be shown that $P(v) = 0.6827$. In other words, the probability that a particular observation will fall within $\pm 1\sigma$ of the mean is 68.27 percent.

Returning to the example of the vessel moored to the offshore platform, the mean and the standard error for the observations are easily computed. With this information and Equation 2.14, the probability of a range error falling within specified limits can be computed. Conversely, by fixing a probability, the associated limits of the range error can be computed. In statistical terms, a particular observation will fall within specified limits with a certain confidence.

Actual values of one-dimensional standard errors for hydrographic positioning equipment are a subject of debate between manufacturers and users. Some manufacturers of microwave positioning equipment claim standard errors of ± 1 meter. On the other hand, Munson [Ref. 9, p. 6] states that microwave systems demonstrate accuracies of 3 meters at short ranges but show larger errors at ranges of 15 km and greater. NOS assumes a 3-meter standard error in all of its short-range accuracy computations. It is apparent that further study is needed to adequately define the nature of errors associated with electronic positioning equipment.

Waltz [Ref. 13] performed an extensive study to determine the pointing error of a Wild T-2 theodolite. His results showed that the pointing error associated with this instrument under hydrographic survey conditions was about 1.3 meters and was independent of distance.

2. Two-Dimensional Errors

The intent of this paper is to apply statistical methods developed by others to a hydrographic data set containing two-dimensional errors which are defined by two random variables. Lengthy and complex derivations are not presented. Burt [Ref. 3] and Heinzen [Ref. 2] show adequate derivations of formulas associated with two-dimensional errors and can be referenced for full details.

The following assumptions are made concerning two-dimensional errors associated with intersecting LOP's:

- i. The random errors of each LOP are normally distributed.
- ii. Systematic or bias errors have been removed from the observations.
- iii. The intersecting LOP's are coplanar.
- iv. The error LOP's are parallel to the exact LOP's.

In developing a usable mathematical model for accuracy determinations, the four assumptions hold to a high degree for all hydrographic positioning geometries.

Consider again the vessel moored to a fixed offshore platform. Assume two ranges are measured from two different shore control stations at the same time and that the range readings are uncorrelated. The observation of this pair of ranges is repeated many times. After a large number of observations, the means and standard errors of the individual ranges are determined. Suppose the mean ranges, or the actual LOP's, intersect at an angle of 90° and that the computed standard errors are equal ($\sigma_1 = \sigma_2$). If each data pair (x_1, y_1) is plotted, the spread of points about the mean coordinates results in a circular cluster (Fig. 2.5). A higher density of points occurs near the intersection of the mean ranges and the density of points decreases outward from the intersection of the mean ranges.

In this special case, which is called a circular normal distribution, the probability of a point falling within a specified radius, R , from the intersection of the mean ranges is

$$P(R) = 1 - e^{-\left(\frac{R^2}{2\sigma^2}\right)} \quad (2.15)$$

where $\sigma_1 = \sigma_2 = \sigma_c$ and is defined as the circular standard error. Using Equation 2.15, R can be computed by fixing P(R), or conversely, P(R) can be computed by fixing R. Letting $R = \sigma_1 = \sigma_2 = \sigma_c$, then $P(R) = 0.3935$. In other words, 39.35 percent of all errors in a circular normal distribution are not expected to exceed the circular standard error [Ref. 12, pp. 25-26].

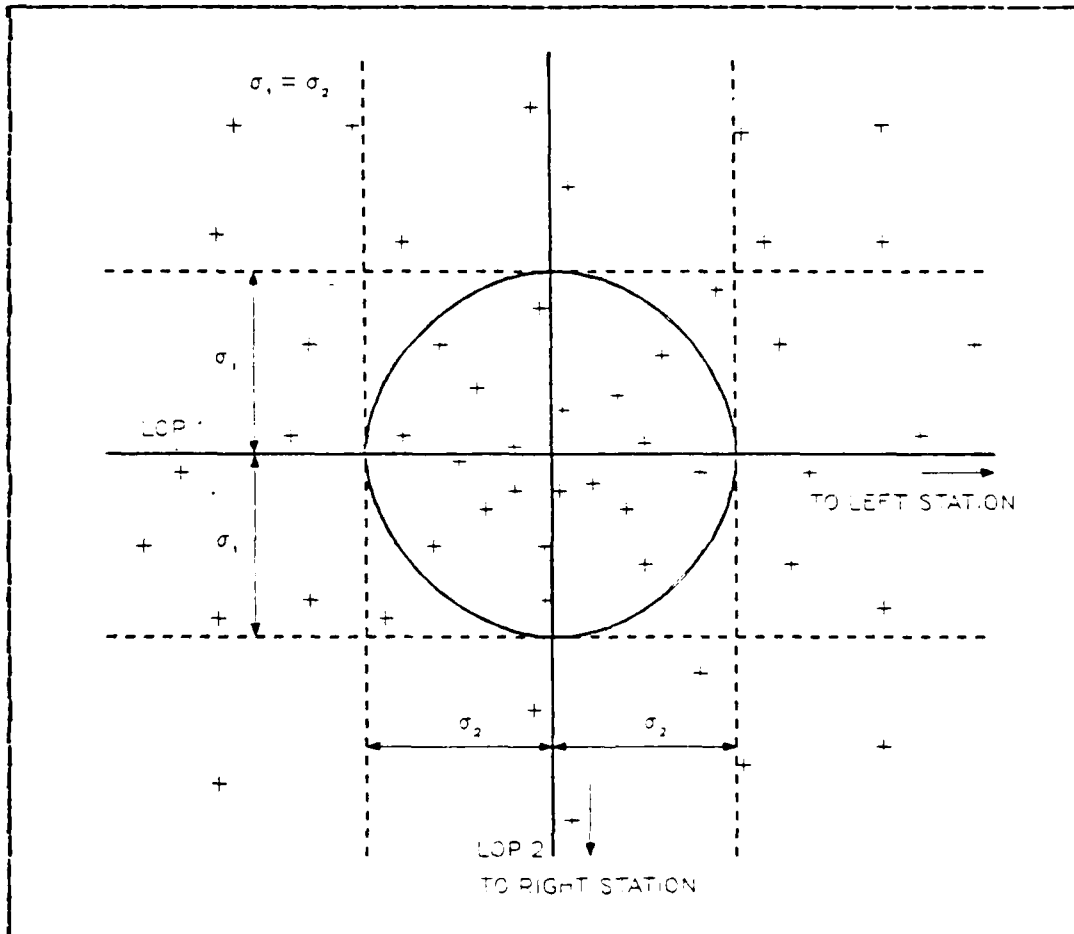


Figure 2.5 Circular Normal Distribution

In the case where the two uncorrelated LCP's intersect at an angle other than 90° or $\sigma_1 \neq \sigma_2$, the contours of

equal density are ellipses centered about the point defined by the intersecting LCP's (Fig. 2.6). The two-dimensional probability density function becomes [Ref. 1, p. 136]

$$P(v_x, v_y) = \frac{1}{2\pi\sigma_x\sigma_y} e^{-\frac{K^2}{2}} \quad (2.16)$$

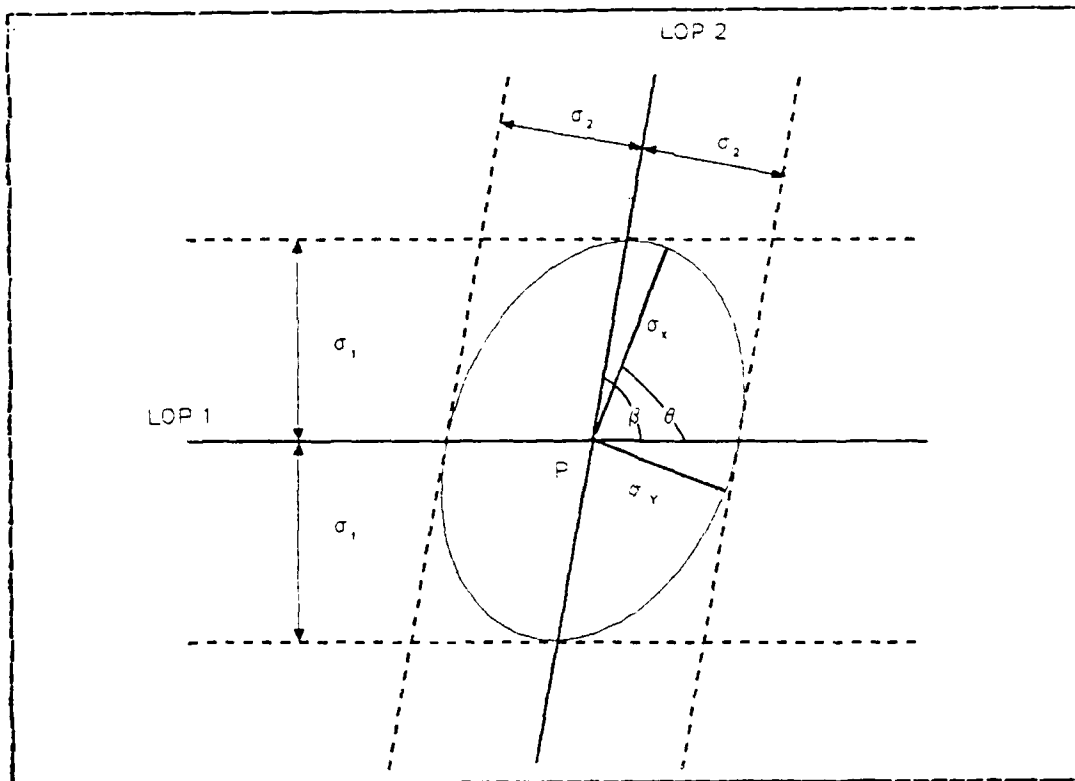


Figure 2.6 Error Ellipse Formed by Two Uncorrelated LCP's

where

v_x is the residual in the direction of the semi-major axis of the error ellipse,

v_y is the residual in the direction of the semi-minor axis,

σ_x is the standard error in the direction of the semi-major axis,

σ_y is the standard error in the direction of the semi-minor axis,

and

$$K^2 = \frac{v_x^2}{\sigma_x^2} + \frac{v_y^2}{\sigma_y^2} \quad (2.17)$$

The solution of Equation 2.16 with values of K for different P's yields the results in Table I [Ref. 12, p. 23]. For a 39.35 percent probability, the axes of the ellipse are $1.0000 \sigma_x$ and $1.0000 \sigma_y$; for a 50 percent probability, the axes are $1.1774 \sigma_x$ and $1.1774 \sigma_y$.

TABLE I	
Values of the Constant K	
<u>PROBABILITY</u>	<u>K</u>
39.35%	1.0000
50.00%	1.1774
63.21%	1.4142
90.00%	2.1460
99.00%	3.0349
99.78%	3.5000

The error ellipse can be used for accuracy computations by developing relationships for σ_x and σ_y in terms of the initial information σ_1 , σ_2 , and β . Bowditch [Ref. 10, p. 1213] gives the following equations for independent IOP's relating these quantities:

$$\sigma_x^2 = \frac{1}{2\sin^2\beta} \left\{ \sigma_1^2 + \sigma_2^2 + \sqrt{(\sigma_1^2 + \sigma_2^2)^2 - 4\sin^2\beta \sigma_1^2 \sigma_2^2} \right\} \quad (2.18)$$

and

$$\sigma_y^2 = \frac{1}{2\sin^2\beta} \left(\sigma_1^2 + \sigma_2^2 - \sqrt{(\sigma_1^2 + \sigma_2^2)^2 - 4\sin^2\beta \sigma_1^2 \sigma_2^2} \right) \quad (2.19)$$

In these equations, β is assumed to be the acute angle between the LOP's.

In certain special cases, the above equations take on more manageable forms. In range-range and azimuth-azimuth positioning it is often assumed that $\sigma_1 = \sigma_2 = \sigma$. Equations 2.18 and 2.19 then reduce to

$$\sigma_x = \frac{\sqrt{2}}{2\sin(\frac{1}{2}\beta)} \sigma \quad (2.20)$$

and

$$\sigma_y = \frac{\sqrt{2}}{2\cos(\frac{1}{2}\beta)} \sigma \quad (2.21)$$

In the concentric range-azimuth case, $\sigma_1 \neq \sigma_2$, and β equals 90° . Equations 2.18 and 2.19 then simplify to

$$\sigma_x = \sigma_1 \quad (2.22)$$

and

$$\sigma_y = \sigma_2 \quad (2.23)$$

where $\sigma_1 > \sigma_2$ and $\sigma_x > \sigma_y$.

The case for correlated LOP's is more complex. The calculation of σ_x and σ_y involves a coordinate transformation from a linear skewed coordinate system to an uncorrelated rectangular coordinate system. The following discussion is taken from Heinzen [Ref. 2, pp. 49-53].

Assume a hydrographic position is established by the intersection of two correlated LOP's (Fig. 2.7a). LOP 1 and

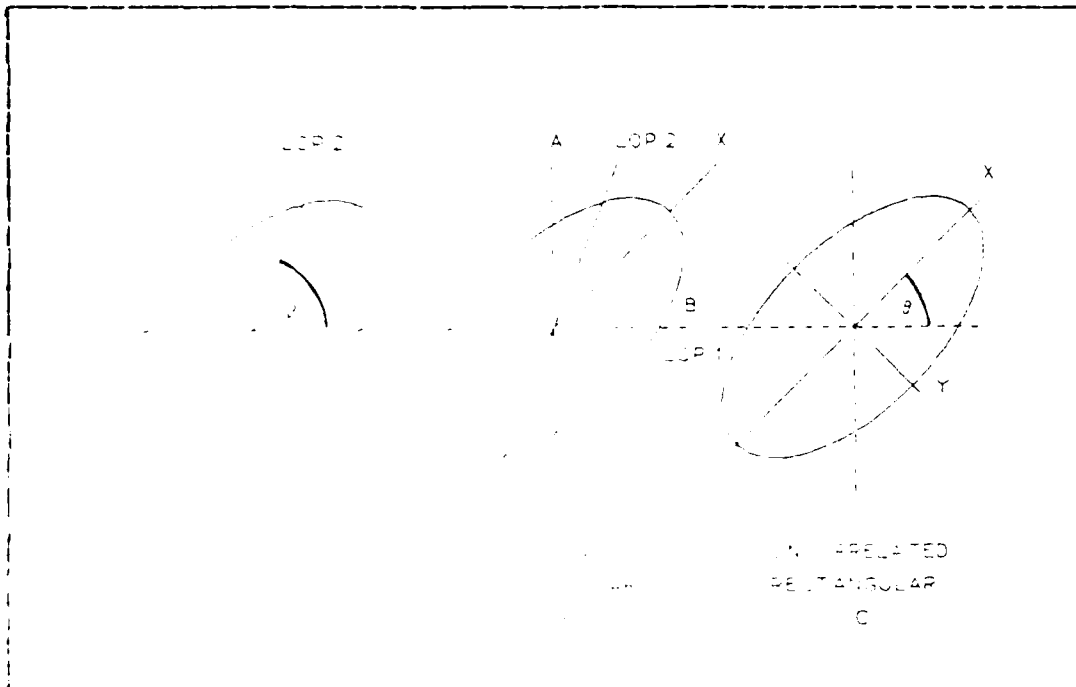


Figure 2.7 Coordinate Transformations for Correlated IOP's

Figure 2.7a shows the IOP axes in the skewed coordinate system, with standard errors σ_1 and σ_2 . The semi-major and semi-minor axes of the error ellipse are not coincident with the skewed coordinate system axes. The correlation coefficient between the two IOP's is ρ_{12} . Assume $\sigma_1 > \sigma_2$.

The standard errors and correlation coefficient in a correlated rectangular coordinate system with axes A and B must now be determined. A coordinate transformation from the skewed system to the correlated rectangular system must be made yielding the standard errors along the new coordinate axes (Fig. 2.7b)

$$\sigma_a^2 = \frac{1}{\sin^2 \beta} (\sigma_1^2 + 2\rho_{12} \sigma_1 \sigma_2 \cos \beta + \sigma_2^2) - \sigma_2^2 \quad (2.24)$$

and

$$\sigma_b = \sigma_2 \quad (2.25)$$

The correlation coefficient in the correlated rectangular system is

$$\rho_{ab} = \left(\frac{\sigma_2}{\sigma_1} \cos\beta + \rho_{12} \right) \left\{ 1 + \rho_{12} \left(\frac{\sigma_2}{\sigma_1} \right) \cos\beta + \left(\frac{\sigma_2}{\sigma_1} \right)^2 \cos^2\beta \right\}^{-1/2} \quad (2.26)$$

To determine σ_x and σ_y , a second coordinate transformation must be performed from the correlated rectangular system to an uncorrelated rectangular system with axes X and Y (Fig. 2.7c). The semi-major and semi-minor axes of the error ellipse are then

$$\sigma_x = \sqrt{\frac{\sigma_a^2 + \sigma_b^2}{2}} \sqrt{1 + \sqrt{1 - \frac{4\sigma_a^2\sigma_b^2(1 - \rho_{ab}^2)}{(\sigma_a^2 + \sigma_b^2)^2}}} \quad (2.27)$$

and

$$\sigma_y = \sqrt{\sigma_a^2 + \sigma_b^2 - \sigma_x^2} \quad (2.28)$$

When $\rho_{12} = 0$, these equations become identical to the simplified versions in Bowditch [Ref. 10].

The orientation of the semi-major and semi-minor axes relative to the intersecting LOP's is the third parameter which fixes the error ellipse. The angle θ (Figs. 2.6 and 2.7) is measured counter-clockwise from LOP 1 to the semi-major axis of the error ellipse [Ref. 11] and is given by

$$\theta = \frac{1}{2} \arctan \left\{ \frac{\sigma_1^2 \sin(2\beta) + 2\rho_{12} \sigma_1 \sigma_2 \sin(\beta)}{\sigma_1^2 \cos(2\beta) + 2\rho_{12} \sigma_1 \sigma_2 \cos(\beta) + \sigma_2^2} \right\} \quad (2.29)$$

For the special case of $\sigma_1 = \sigma_2$ and $\rho_{12} = 0$,

$$\theta = \frac{\beta}{2} \quad (2.30)$$

The orientation of the error ellipse in an orthogonal coordinate system can be represented by adding or subtracting θ to the orientation of LCP 1. Care must be taken on determining the quadrant of the outcome. As a general rule, the error ellipse always lies within the acute angles formed by the intersecting LOP's.

The orientation and dimensions of the error ellipse provide a useful index for evaluating the accuracy of a hydrographic position. Its greatest attribute is that it accurately represents the error distribution about the intersection of two LCP's in terms of a fixed probability. It is interesting to examine the variation in the relative dimensions and orientations of error ellipses as they vary in a range-range configuration with $\sigma_1 = \sigma_2 = \sigma$ (Fig. 2.8). The dimensions of the ellipses are specified by Equations 2.20 and 2.21 and σ_x and σ_y are functions of β only for fixed σ . Therefore, the dimensions of the ellipses remain constant along a contour of constant β ; only the orientation changes. A line of constant β is a circle which includes stations L and E. Note that the dimensions of the ellipses for β 's of 30° and 150° are identical. The ellipses about the 90° angle of intersection contour are circles and represent the strongest possible positions in this scheme. With varying β 's, the directional nature of the distribution can be noted.

3. Circular Precision Indexes

Although the error ellipse gives a true representation of the error distribution about a hydrographic position, its use has certain drawbacks. The characteristics of the ellipse must be specified by the three quantities σ_x , σ_y , and θ . A single figure for evaluating the positional accuracy cannot be used. Greenwalt [Ref. 12, p. 26] states that when σ_x and σ_y are not equal, a circular error

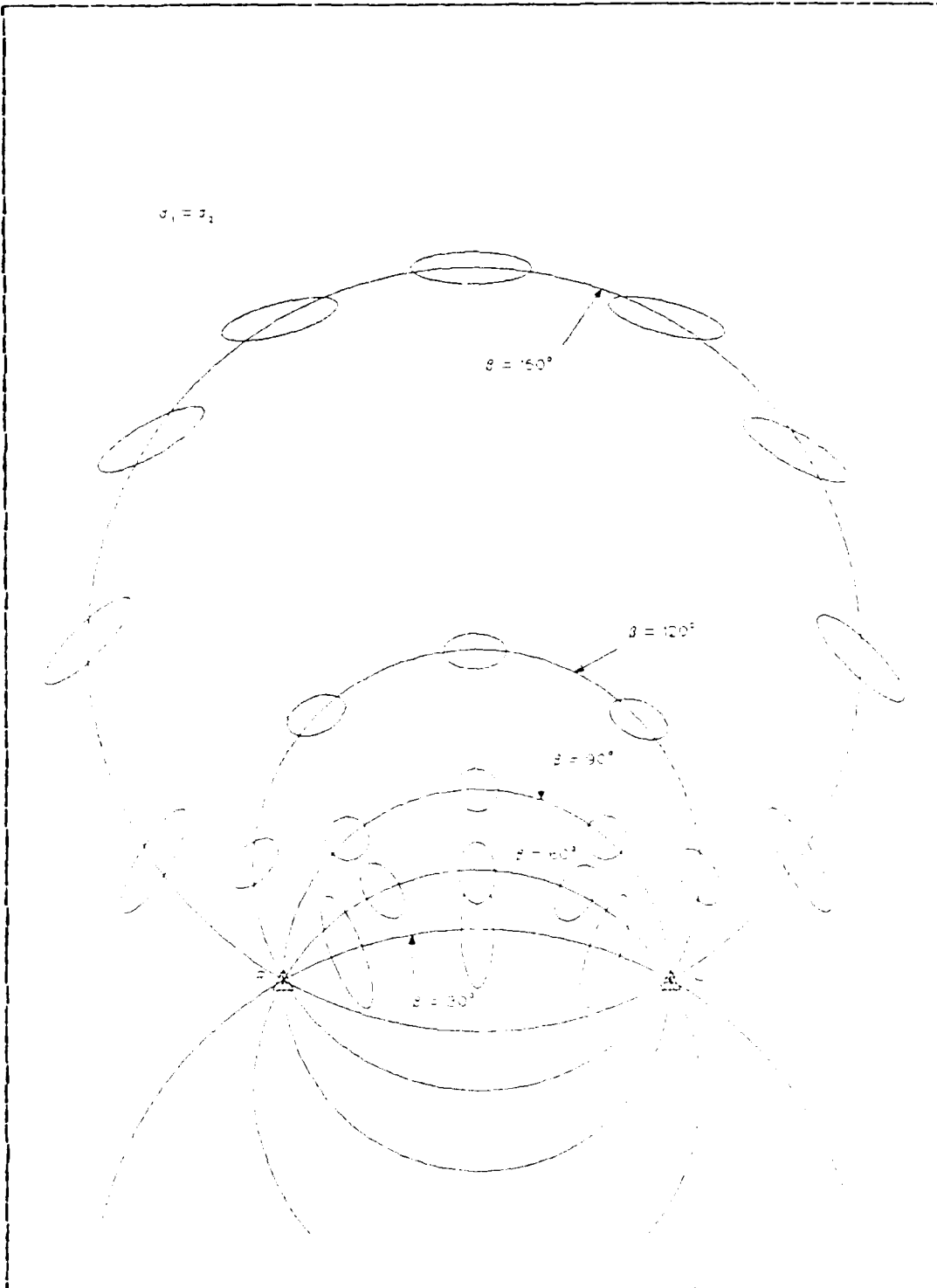


Figure 2.8 Error Ellipses Around a Range-Range System

TABLE V
Coordinates of Control Stations

<u>STATION NAME</u>	<u>GEODETTIC COORD.</u>	<u>MTM COORD.</u>
USE MON	360 36' 04.685" N 1210 52' 35.900" W	Y = 1982.43 m. X = 4853.36 m.
MUSSEL	360 37' 18.151" N 1210 54' 11.628" W	Y = 4247.42 m. X = 2474.75 m.
FEACH LAB	360 36' 05.571" N 1210 52' 33.427" W	Y = 2009.86 m. X = 4914.75 m.

B. ACCURACY ANALYSIS OF HYDROGRAPHIC POSITIONING DATA

The objective of this section is to illustrate how the accuracy of hydrographic positioning data can be classified using Furt's method of circles of equivalent probability. The radius of the 90 percent confidence circle was computed for each position; it provides a quantitative measure of repeatable accuracy.

For subsequent accuracy computations, the following assumptions were made:

- i. The standard error for the microwave ranging system used in the range-range and range-azimuth computations is 3 meters.
- ii. For azimuth-azimuth and range-azimuth positions, the pointing error of the theodolite is 1.3 meters at all ranges.
- iii. The two LOP's involved in all types of positioning are independent ($\rho_{12} = 0$).
- iv. The data are free of systematic errors.

Raw range and azimuth data were hand logged into a data file for processing. A modification of program UCOMPS was

IV. RESULTS AND DATA ANALYSIS

A. DATA PROCESSING

Automated processing of the positional survey data was done on the NPS IBM 370/3033AP computer system. Graphic displays were constructed using the Display Integrated Software System and Plotting Language (DISSPLA) developed by the Integrated Software Systems Corporation (ISSCO) [Ref. 16]. All computer programs involved in data processing were written in the WATFIV programming language.

Computations were made in an X-Y coordinate system based on a Modified Transverse Mercator (MTM) projection. A MTM projection is essentially the same as a Universal Transverse Mercator (UTM) projection, the only difference being that in a MTM projection a central meridian is picked near the survey area instead of being fixed at a particular meridian [Ref. 17].

The central meridian, controlling latitude, and false easting values define the coordinate system used for computations. The central meridian for the projection was chosen to be longitude $121^{\circ} 52' 30''$ W which is approximately the mean longitude of the survey area. The controlling latitude, the distance in meters from the equator to a reference latitude, was chosen to be 4,050,000 meters. A false easting of 5,000 meters was chosen as the value of the X-coordinate at the central meridian.

Three shore control stations were used in the acquisition of survey data. The geodetic positions of these stations were converted to the X-Y coordinate system (Table V) using program UCOMPS, which is a hydrographic utility package available to students at NPS.

Range information was recorded using a Racal Decca Trisponder system, a microwave system commonly used for nearshore, line-of-sight survey work. On October 28 and November 30, range-range data were recorded by setting remote units over stations BEACH LAB and MUSSEL. Before and after the survey, the ranging system was calibrated over the fixed base line USE MCN to MUSSEL. Daily checks in the survey area were made to determine if the system was working properly. This was accomplished by maneuvering the survey vessel to a point where two known navigational ranges intersected. One navigational range was formed by stations MONTEFEY AMERICAN CAN COMPANY STACK and MONTEREY RADIO STATION KMBY MAST. A second navigational range was formed by stations MONTEREY HARBOR LIGHT 6 and MONTEREY BLUE LIGHTHOUSE.

Track control for range-azimuth and range-range positions was accomplished by steering the vessel along range arcs. The spacing between range arcs for most lines was planned to be 40 meters. Distance between positions along a sounding line averaged approximately 200 meters. The azimuth-azimuth lines were controlled by steering a magnetic compass heading.

The data acquired under training conditions contained several deficiencies that would normally not be tolerated. For example, the quality of the line steering was generally poor; the vessel wandered off the arc more than 10 meters in several instances. The quality of the sounding lines run using azimuth-azimuth control was extremely deficient; the position plot of these lines show a jagged path by the vessel. Under normal hydrographic procedures, these positions would be rejected. Since the intent of this study is to demonstrate accuracy analysis techniques, these deficiencies prove to be inconsequential; the acquired data are adequate to demonstrate the concepts.

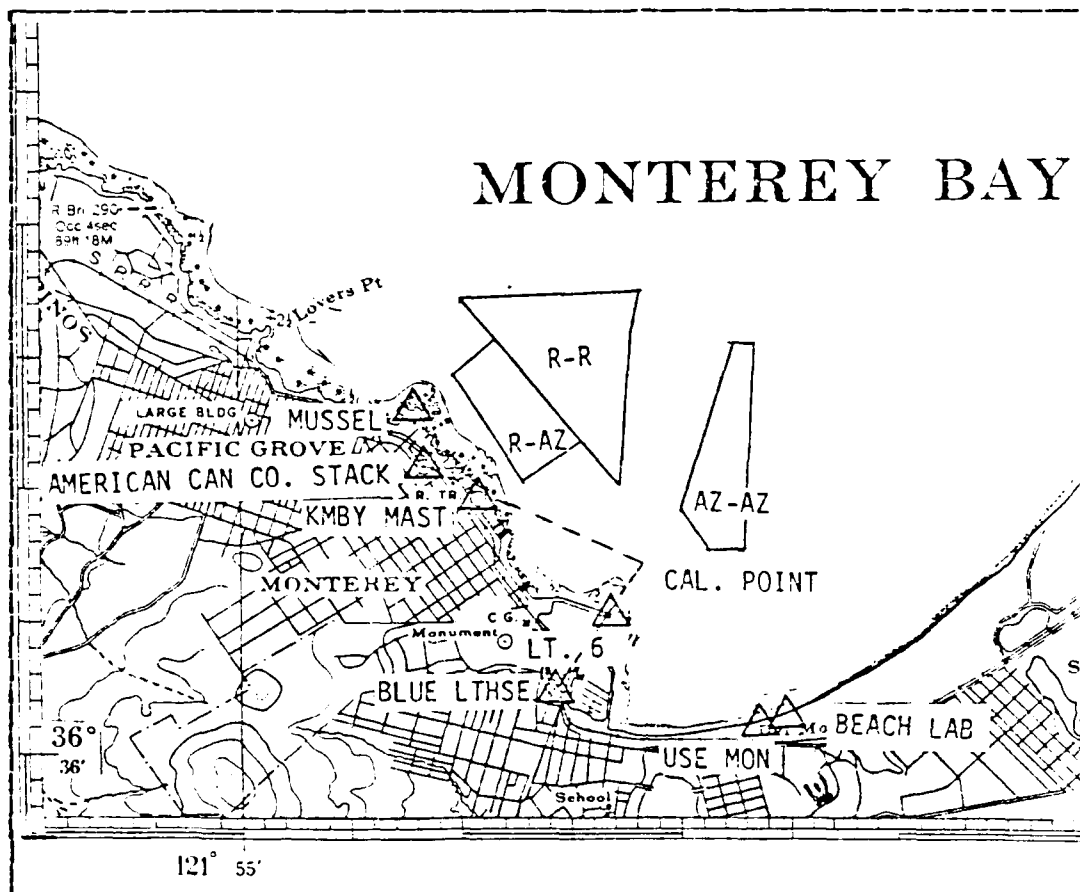


Figure 3.1 Hydrographic Survey Area

all stations are of third-order or better and are published in the National Geodetic Survey Data Base.

For azimuth-azimuth and range-azimuth positioning, azimuths were measured with a Wild T-2 theodolite. On November 16, range-azimuth information was acquired by locating the theodolite over station MUSSEL and initialing on USE MCN. The initial direction was checked by sighting on KMBY MAST. Azimuth-azimuth positions were acquired on November 23. A theodolite was set over USE MON and an initial direction was to MUSSEL. A second theodolite was set at MUSSEL using USE MON for the initial direction.

III. EXPERIMENT DESIGN AND IMPLEMENTATION

The goals of this chapter are to demonstrate that hydrographic positioning accuracy can be classified based on the radii of 90 percent confidence circles determined by using Eurt's method and to show that, based on the same criteria, accuracy predictions can be made for survey planning purposes.

A. DATA ACQUISITION PROCEDURES

The data used for analysis and prediction consisted of range-range, azimuth-azimuth and range-azimuth survey information. The data were acquired by Naval Postgraduate School (NPS) students in a Hydrographic Sciences course. Although the course was structured as a training exercise, the data acquisition procedures utilized were nearly identical to those which are practiced by NOS.

A total of 453 hydrographic positions were recorded during the survey of a nearshore area in southern Monterey Bay, California. Of the positions used for analysis, 292 were range-range, 81 were range-azimuth, and 80 were azimuth-azimuth. All survey information was recorded by hand in sounding volumes. The vessel used was a 36-foot Uniflite with a fiberglass hull and twin engines. The survey was conducted on October 28, November 16, 23, and 30, 1983. Electronic control and calibration stations used for the survey included USE MON 1978, MUSSEL 1932, BEACH LAB 1982, MONTEREY AMERICAN CAN COMPANY STACK 1932, MONTEREY RADIC STATION KMBY MAST 1962, MONTEREY HARBOR LIGHT 6 1978, and MONTEREY BLUE LIGHTHOUSE (Fig. 3.1). With the exception of MONTEREY BLUE LIGHTHOUSE, which is a low-order position,

Given the frequency of 1.6 MHz, $\lambda = 187.37$ meters from Equation 2.3. The lane width along the base line is $w'_g = w'_r = 93.68$ meters from Equation 2.5. Using the law of cosines from plane geometry, the subtended angles α_g and α_r are 32.47° and 43.25° , respectively. The angle of intersection of the two hyperbolas at P is 37.86° from Equation 2.7. The lane widths at P are $w_r = 254.19$ meters and $w_g = 335.06$ meters from Equation 2.6. The standard errors of the green (σ_1) and red (σ_2) hyperbolas, respectively are $\sigma_1 = w_g \sigma_{g \text{ base}} = 16.7$ meters and $\sigma_2 = w_r \sigma_{r \text{ base}} = 12.7$ meters. These standard errors are in a linear skewed coordinate system and must be transformed to an uncorrelated rectangular system. From Equations 2.18 and 2.19, the values of σ_a and σ_b are 36.9 meters and 12.7 meters, respectively. The correlation coefficient in the correlated rectangular system (ρ_{ab}) is then 0.737 from Equation 2.26. The semi-major and semi-minor axes in the uncorrelated rectangular system are 38.1 meters and 8.3 meters, respectively, from Equations 2.27 and 2.28. The eccentricity is

$$c = \frac{\sigma_y}{\sigma_x} = 0.218$$

Table IV is entered with the values of $P = 0.9$ and $c = 0.218$. The value for K is found to be

$$K = 1.6602$$

From Equation 2.37, the radius of the 90 percent probability circle is found to be

$$R = 63.3 \text{ meters}$$

The probability that the vessel's position will be within a circle of 63.3-meter radius centered at the intersection of the LCP's is 90 percent.

then $\sigma_x = \sigma_y = 1.3$ meters

$$c = \frac{\sigma_y}{\sigma_x} = 0.433$$

Table IV is entered with the values of $P = 0.9$ and $c = 0.433$. The value for K is found to be

$$K = 1.7117$$

Using Equation 2.37, the radius of the 90 percent probability circle is found to be

$$R = 5.14 \text{ meters}$$

The probability that the vessel's position will be within a circle of 5.14-meter radius centered at the intersection of the LCP's is 90 percent.

Example 3

A vessel is conducting a hydrographic survey using hyperbolic-hyperbolic geometry. The hyperbolic LCP generated by the 1.6-MHz electronic positioning system has a standard error of 0.05-lane on the base line. The correlation coefficient (ρ) between the two LCP's is known to be 0.4. Compute the radius of the 90 percent confidence circle at the vessel's position.

The rectangular plane coordinates of the master (M), two slaves (G and P), and the vessel's position (P) are

	<u>X COORDINATE</u> (m)	<u>Y COORDINATE</u> (m)
P	172,679.1	62,540.4
G	308,679.1	98,540.4
M	241,738.2	21,325.4
P	223,172.5	169,264.2

Example 1

A vessel is conducting a hydrographic survey using range-range geometry. The two LOP's generated by microwave transmitters have standard errors of $\sigma_1 = 3$ meters and $\sigma_2 = 4$ meters. The angle of intersection β at the vessel is 30° . Assume the LOP's are uncorrelated. Compute the probability that the vessel's position will be within a circle of 10-meter radius with the center at the intersection of the LOP's.

Recalling Equations 2.18 and 2.19, the values of σ_x and σ_y are found to be 9.79 meters and 6.14 meters, respectively. From Equation 2.36

$$c = \frac{\sigma_y}{\sigma_x} = 0.633$$

and from Equation 2.37, with $R = 10$ meters,

$$K = 1.032$$

Entering Table III and using interpolated values for c and K , the probability that the vessel's position will be within a circle of 10-meter radius centered at the intersection of the LOP's is

$$P = 53.2\%$$

Example 2

A vessel is conducting a hydrographic survey using range-azimuth geometry. The range LOP generated by the microwave transmitter has a standard error of 3 meters. The azimuth LOP determined by theodolite observation has a standard error of 1.3 meters at all ranges. Compute the radius of the 90 percent confidence circle at the vessel's position.

In the range-azimuth case $\beta = 90^\circ$ and the LOP's are uncorrelated. Therefore,

$$\sigma_1 = \sigma_x = 3.0 \text{ meters}$$

and

TABLE IV
Radii of Circles Given c and P

P \ c	c										
	0.0	0.1	0.2	0.3	0.4	0.5	0.6	0.7	0.8	0.9	1.0
5000	0.67449	0.88199	0.70585	0.74993	0.80785	0.87042	0.93365	0.99621	1.05769	1.11807	1.17741
7500	1.15035	1.15473	1.16825	1.17446	1.23100	1.25134	1.35143	1.42471	1.50231	1.55271	1.65111
9000	1.64465	1.64791	1.65731	1.67043	1.69918	1.73708	1.79152	1.86253	1.94761	2.04236	2.14597
9500	1.85986	1.86253	1.87041	1.88420	2.00514	2.03556	2.08130	2.14798	2.23029	2.33180	2.44775
1750	2.24140	2.24365	2.25051	2.26235	2.28073	2.30707	2.34581	2.40356	2.48494	2.58999	2.71620
9900	2.57583	2.57778	2.58377	2.59421	2.60935	2.63257	2.66533	2.71515	2.79069	2.89743	3.03485
9950	2.80703	2.80883	2.81432	2.82289	2.83430	2.85594	2.88559	2.93347	3.00431	3.11673	3.25325
9975	3.02154	3.02290	3.03010	3.03895	3.05274	3.07144	3.09871	3.13669	3.20546	3.31099	3.45164
9990	3.29053	3.29208	3.29673	3.30489	3.31715	3.33494	3.35949	3.39647	3.45598	3.55939	3.71692

confidence ellipse is

$$A_e = K \sigma_x^2 \sigma_y^2 \pi \quad (2.38)$$

where K is the appropriate probability conversion factor (Table I). The area of the 90 percent confidence circle is

$$A_c = \pi R^2 \quad (2.39)$$

where R is given by Equation 2.37. For a condition where $\sigma_1 = \sigma_2 = 3$ meters, and $\beta = 30^\circ$, the area of the 90 percent confidence ellipse is 261 square meters, while the area of the confidence circle is 587 square meters. For both standard errors equaling 10 meters and $\beta = 30^\circ$, the 90 percent confidence ellipse has an area of 921 square meters and the confidence circle has an area of 2894 square meters. From an operational perspective, the difference in areas between ellipses and circles have significant implications which will be discussed in Chapter V.

The following examples are presented to demonstrate methods for computing the parameters of error ellipses and confidence circles for several hydrographic positioning geometries.

b. Circles of Equivalent Probability

Burt [Ref. 3] presents a method for translating ellipses of equivalent probability into circles of equivalent probability. To utilize this method, it is first necessary to compute the eccentricity of the error ellipse, c , by the equation

$$c = \frac{\sigma_y}{\sigma_x} \quad (2.36)$$

where $\sigma_x > \sigma_y$.

Harter [Ref. 15] compiled Tables III and IV which are taken from Bowditch [Ref. 10, p. 1215]. Harter's data are given in terms of the eccentricity, c , a parameter, K , and a probability, P . The parameter, K , when multiplied by σ_x gives the value of the radius, R , of the circle of the corresponding probability shown in Table III. That is,

$$R = K \sigma_x \quad (2.37)$$

The probability of a point falling inside a circle of specified radius can be computed by entering Table III with c and K as arguments. Given a fixed probability, K is determined by entering Table IV using c and P as arguments. The radius of the probability circle is then computed using Equation 2.37.

Using confidence ellipses has certain advantages over confidence circles of equal probability. First, the directional nature of the true error distribution is not represented in the confidence circle method even though both methods give an accurate measure of confidence. Second, the area of the confidence ellipse is always less than or equal to the area of the confidence circle. The area of a

- i. 0.5 mm at the scale of the survey for scales of 1:20,000 and smaller,
- ii. 1.0 mm at the scale of the survey for 1:10,000 scale surveys, or
- iii. 1.5 mm at the scale of the survey for scales of 1:5,000 and larger.

The major advantage of using d_{rms} as a precision index is its ease of computation. Some hydrographers draw analogy between the varying probability associated with one d_{rms} (63.2 percent to 68.3 percent) and the fixed probability associated with a one-dimensional standard error (68.3 percent). In fact, d_{rms} has very little statistical meaning. The obvious problem with using d_{rms} as a precision index is the varying probability associated with the error circle. For this reason Greenwalt [Ref. 12, p. 31] recommends against its use.

TABLE II
Probabilities Associated With d_{rms}

σ_y	σ_x	LENGTH OF $1 d_{rms}$	PROBABILITY	
			$1 d_{rms}$	$2 d_{rms}$
0.0	1.0	1.000	0.683	0.954
0.1	1.0	1.005	0.682	0.955
0.2	1.0	1.020	0.682	0.957
0.3	1.0	1.042	0.676	0.961
0.4	1.0	1.077	0.671	0.966
0.5	1.0	1.118	0.662	0.969
0.6	1.0	1.166	0.650	0.973
0.7	1.0	1.220	0.641	0.977
0.8	1.0	1.280	0.635	0.980
0.9	1.0	1.345	0.632	0.981
1.0	1.0	1.414	0.632	0.982

An error circle with a radius of one d_{rms} can be constructed about the intersecting LOP's (Fig. 2.9). Two d_{rms} is the radius of the error circle obtained using two times the values of σ_x and σ_y in Equation 2.31. For an elliptical error distribution, the probability associated with a specific value of d_{rms} varies as a function of the eccentricity of the error ellipse (Table II). The probability associated with one d_{rms} varies from 63.2 percent to 68.3 percent, while the probability associated with two d_{rms} varies between 95.4 percent and 98.2 percent.

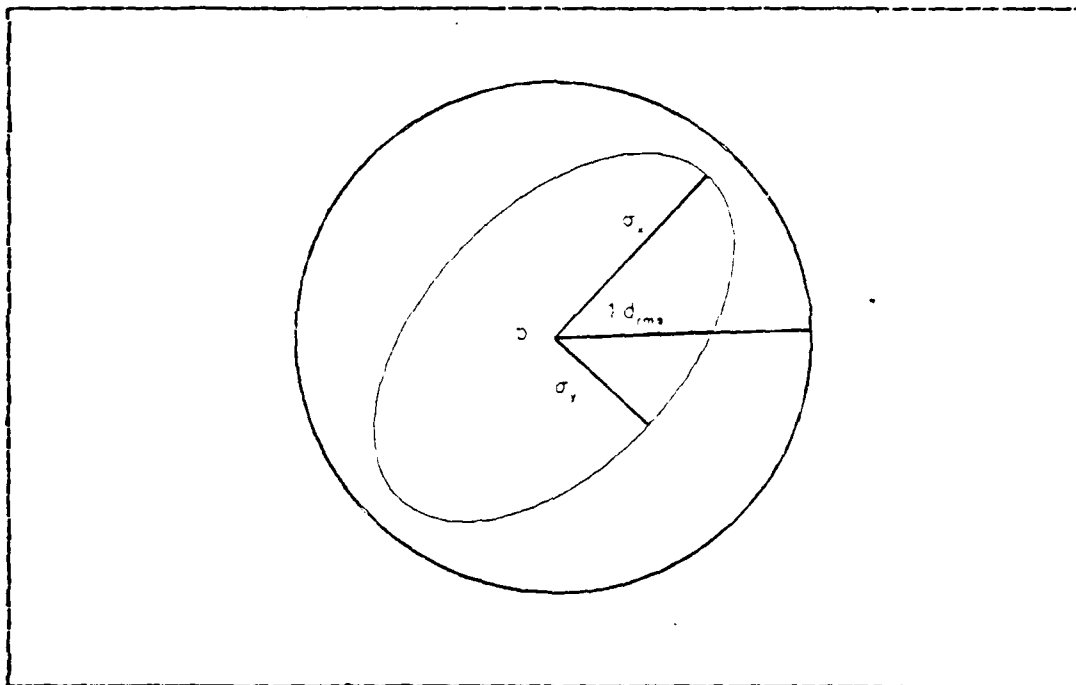


Figure 2.9 The d_{rms} Error Circle

NOS uses d_{rms} as an accuracy specification. Umbach [Ref. 14, p. 4-25] states that super high frequency direct distance measuring systems would be used only when the value of d_{rms} is less than or equal to:

distribution can be substituted for the elliptical distribution. This substitution can be satisfactory for error analysis within certain σ_y/σ_x ratios. However, when this ratio is small the distortion introduced by the circular distribution may become misleading.

a. Root Mean Square Error

The terms radial error, root mean square error, and d_{rms} are identical in meaning when applied to two-dimensional errors [Ref. 10, p. 1229]. The term d_{rms} is defined as the square root of the sum of the squares of the standard errors along the major and minor axes of the error ellipse. That is

$$d_{rms} = \sqrt{\sigma_x^2 + \sigma_y^2} \quad (2.31)$$

where σ_x and σ_y are given by Equations 2.18 and 2.19. A more direct form of 2.31 is given by [Ref. 2, p. 54]

$$d_{rms} = \frac{1}{\sin \beta} \sqrt{\sigma_1^2 + \sigma_2^2} \quad (2.32)$$

for uncorrelated LOP's. For range-range and azimuth-azimuth positioning, with $\sigma_1 = \sigma_2 = \sigma$, Equation 2.32 reduces to

$$d_{rms} = \frac{\sqrt{2}}{\sin \beta} \sigma \quad (2.33)$$

For range-azimuth positioning, $\beta = 90^\circ$ and Equation 2.32 becomes

$$d_{rms} = \sqrt{\sigma_1^2 + \sigma_2^2} \quad (2.34)$$

The more general form of Equation 2.32 for both correlated and uncorrelated LOP's [Ref. 2, p. 59] is

$$d_{rms} = \frac{1}{\sin \beta} \sqrt{\sigma_1^2 + \sigma_2^2 + 2\rho_{12} \sigma_1 \sigma_2 \cos \beta} \quad (2.35)$$

where ρ_{12} is the correlation coefficient.

used to compute X-Y coordinates of all positions. Based on geometric relationships discussed earlier, angles of intersection of the LCP's were then computed for range-range and azimuth-azimuth points. The angles of intersection for all range-azimuth positions are 90° .

The range-range and azimuth-azimuth data were then passed to WATFIV subroutine PRCB (Appendix A). As input parameters, the subroutine accepts two standard errors of the LCP's and the corresponding angle of intersection. The output parameters include the semi-major and semi-minor axes of the 90 percent confidence ellipse, the radius of the 90 percent confidence circle, and the areas covered by both figures.

Subroutine PROB uses a linear approximation to determine the value of the function K for varying values of the eccentricity, c , in Burt's method. A linear interpolation was performed by first taking the eleven discrete values of c and K for a probability of 90 percent from Table IV and then constructing a series of relationships for K as a function of c (Table VI).

Values of the radii of 90 percent confidence circles for range-range data were plotted at their respective positions (Fig. 4.1). The arcs of circles connecting the two control stations BEACH LAB and MUSSEL represent lines of constant intersection angle (30°). Of the range-range data set, position 848 (Appendix B)--coordinates $X = 4119.01$, $Y = 4735.07$ --was found to have the smallest radius (strongest position) of 6.4 meters and an angle of intersection of 90.2° . Position 137--coordinates $X = 3345.86$, $Y = 3873.34$ --represents the weakest position with radius value of 15.3 meters and an angle of intersection of 26.7° .

The positional accuracy degrades rapidly as the intersection angle approaches 30° ; the 30° arc represents a line of constant 13.7 meter radius. Within 400 meters of the 30°

TABLE VI
Linear Approximations for K as a Function of c

<u>Interval of c</u>	<u>Linear Interpolation Function for K</u>
0.0 - 0.1	K = .0306c + 1.64485
0.1 - 0.2	K = .0940c + 1.63851
0.2 - 0.3	K = .1652c + 1.62427
0.3 - 0.4	K = .2535c + 1.59778
0.4 - 0.5	K = .3790c + 1.54758
0.5 - 0.6	K = .5444c + 1.46488
0.6 - 0.7	K = .7101c + 1.36546
0.7 - 0.8	K = .8508c + 1.26697
0.8 - 0.9	K = .9475c + 1.18961
0.9 - 1.0	K = 1.0361c + 1.10987

intersection arc, the radius varies between 8 and 15 meters. The radii values change slowly in the vicinity of the minimum value of 6.4 meters which corresponds to an angle of intersection of 90°.

The radii of 90 percent confidence circles associated with the azimuth-azimuth positions acquired using control stations USE MON and MUSSEL were also plotted at their respective positions (Fig. 4.2). The standard errors of the LOP's are assumed to be 1.3 meters; the resulting improved accuracy is evident. The maximum value of the 90 percent confidence circle radii is 8.7 meters at position 637--coordinates X = 4327.25, Y = 2818.39--which corresponds to an angle of intersection of 159.8° (or in terms of the supplement, 20.2°). Position 682--coordinates X = 4611.20, Y = 4421.29--represents the strongest position recorded during the survey with a 90 percent confidence circle radius of 2.8 meters and an angle of intersection of 91.0°.

Again, the rapid degradation of accuracy is noted approaching $\theta = 150^\circ$. The arc of the 150° intersection angle represents a constant radius of 5.9 meters. Discrete

SURVEY DATA ANALYSIS R/R

RADII OF 90% PROBABILITY CIRCLES

STATIONS BEACH LAB AND MUSSEL

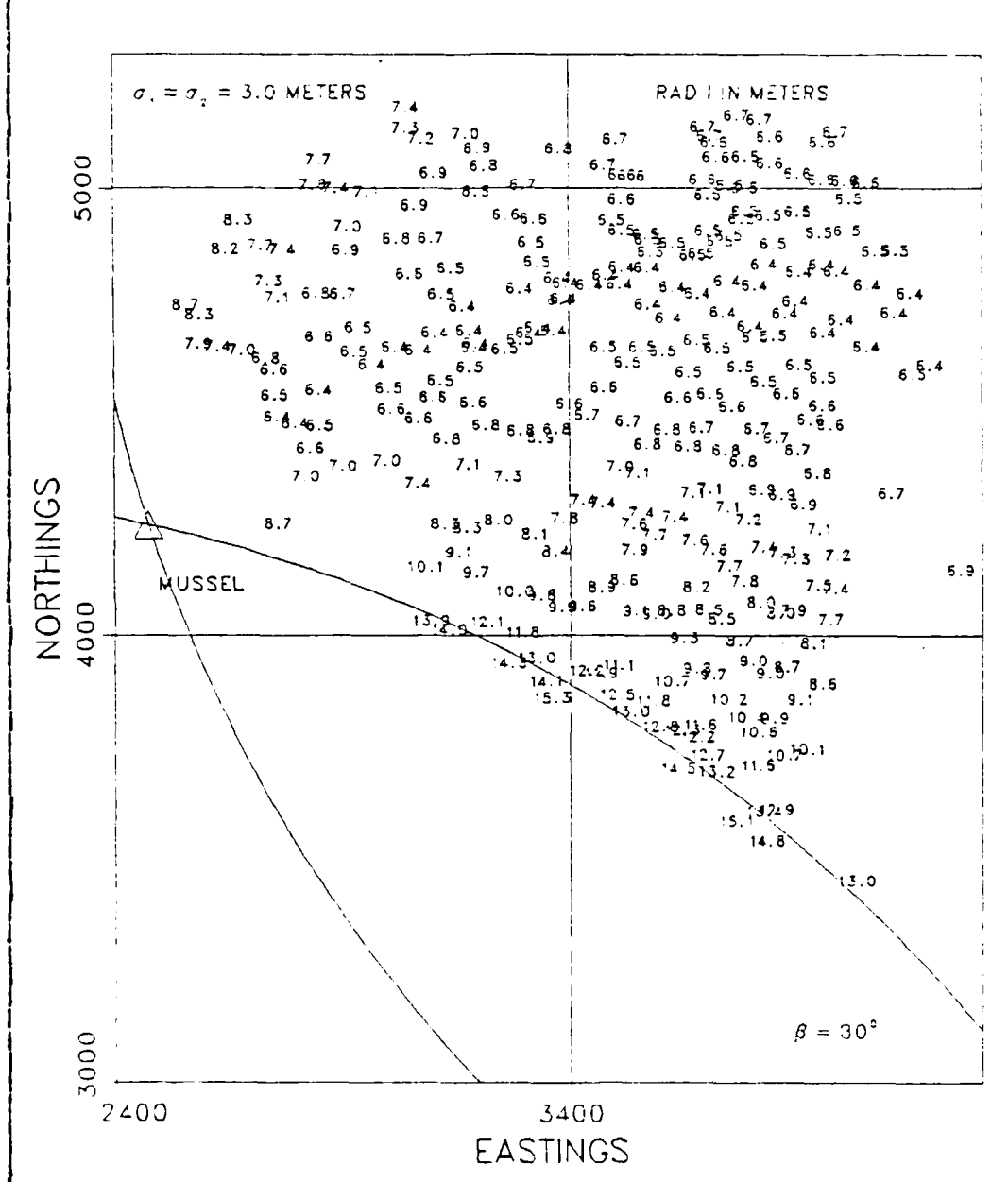


Figure 4.1 Range-Range Accuracy Analysis

SURVEY DATA ANALYSIS AZ/AZ
 RADIi OF 90% PROBABILITY CIRCLES
 STATIONS USE MON AND MUSSEL

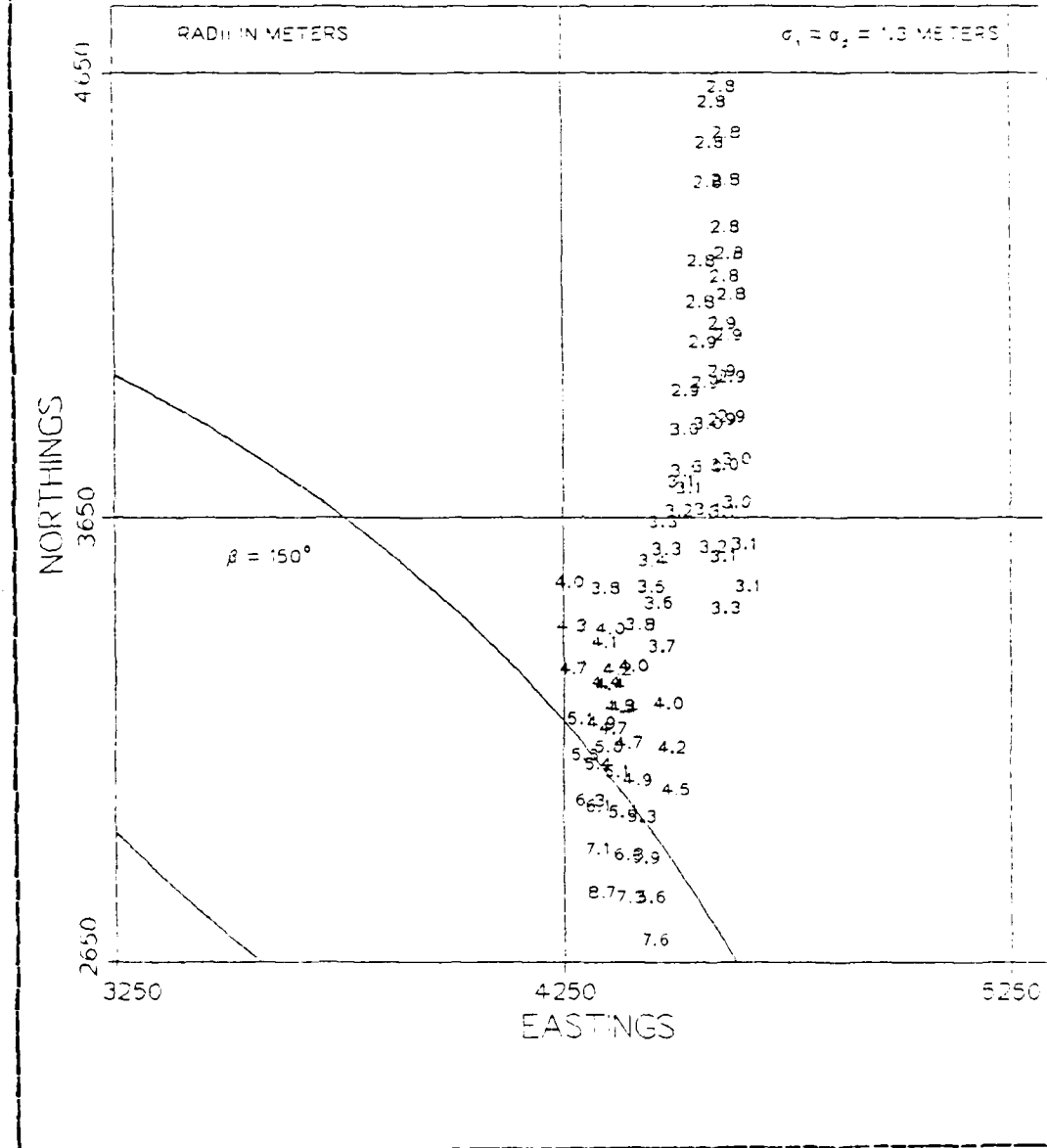


Figure 4.2 Azimuth-Azimuth Accuracy Analysis

values along the arc confirm this qualitatively. A large area of strong positional accuracy surrounds the area where $\beta = 90^\circ$. Numerous values of 2.8 meters are present near the top of the plot.

Using the assumptions stated at the beginning of this section, the values for all radii of 90 percent confidence circles for range-azimuth positions are 5.1 meters. This computation was carried out in Example 2 of Chapter II. Since this case is trivial, the data are not displayed graphically.

Positioning data were also classified based on the parameters of the 90 percent confidence ellipse. WATFIV program ELLIP (Appendix C) was used to generate the parameters of the 90 percent confidence ellipse for range-range, azimuth-azimuth, and range-azimuth positioning data. The program was initialized by entering the coordinates of the control stations and standard errors of the LOP's. The fix number, hydrographic position coordinates, and angle of intersection were then read in from a data file. Subroutine PROB was called to compute values for $K\sigma_x$ and $K\sigma_y$.

The angle of orientation of the major axis of the ellipse, measured clockwise from north, was then computed. For range-range and azimuth-azimuth positions, the LCP generated from the left control station was used as the base LOP. For range-azimuth positions, the LOP formed by the theodolite was used as the base LOP. First, the orientation of the base LOP in the coordinate system was determined. The orientation of the major axis of the error ellipse relative to the base LOP (θ) was then computed using Equation 2.29. By adding or subtracting θ to the orientation of the base LOP, the orientation of the major axis of the error ellipse in the coordinate system was determined. This angle takes on values from 0° to 180° . Appendix D consists of the confidence ellipse classification scheme for range-range,

azimuth-azimuth and range-azimuth data. Forty positions for each positioning geometry are listed for comparison to the classification scheme presented in Appendix B.

Appendix B lists the data by position number, X-Y coordinate, angle of intersection, and radius of the 90 percent confidence circle. Appendix D lists the data by position number, X-Y coordinate, angle of intersection, $K\sigma_x$, $K\sigma_y$, and angle of orientation for the 90 percent confidence ellipse. These appendices are similar to hydrographic survey data bases and demonstrate accuracy classification schemes based on the two criteria.

C. ACCURACY PREDICTIONS

The overall positional accuracy of a survey can be controlled by computing accuracy values before data acquisition is begun. For example, if the hydrographer is using radii of 90 percent confidence circles as an accuracy criterion, the minimum allowable angle of intersection for two LCP's can be computed for meeting specifications. The nature of the survey area may allow the flexibility to change system geometry to maximize accuracy at a specific location or to maximize the area covered with a given accuracy. By making accuracy computations before acquiring data, the hydrographer may also have the option of deciding what type of positioning system is to be used to meet accuracy requirements.

The construction of reliability contours is one method to display the expected positional accuracy. Reliability contours, lines of constant repeatable accuracy which are functions of the system geometry and standard errors of the positioning equipment, can be constructed about shore stations using the radii of 90 percent confidence circles criterion or the less desirable d_{rms} value.

Consider the equations that have been developed in Chapter II for the determination of radii of 90 percent confidence circles using Burt's method. For uncorrelated LOP's in a range-range or azimuth-azimuth system, the repeatable accuracy of a hydrographic position is a function only of the angle of intersection, assuming the standard errors of the LOP's are constant throughout the survey area. The locus of points which define a constant angle of intersection for two LOP's in a range-range or azimuth-azimuth system is a circle which passes through both control stations. Given the coordinates of the two control stations, the equations of these circles can be determined.

Construction of reliability contours involves several simple trigonometric relationships (Fig. 4.3). Let LR be the line connecting the two shore control stations L and R in a range-range system. The length of line LR is b. The circle through both stations defines a line of constant intersection angle for two LOP's. The radius of the circle is r. The distance e is measured along the perpendicular bisector of the line LR to the center of the circle at point O (h,k) and is given by

$$e = \frac{b}{2 \tan \theta} \quad (4.1)$$

Knowing e and the radius r, the coordinates of point O can be computed. The equation of the circle is then

$$r^2 = (x - h)^2 + (y - k)^2 \quad (4.2)$$

These two equations were used to generate reliability contours for display on a computer graphics terminal. Using Burt's method, the angles of intersection of two LOP's were computed for discrete values of radii of 90 percent confidence circles. Reliability contours about stations BEACH

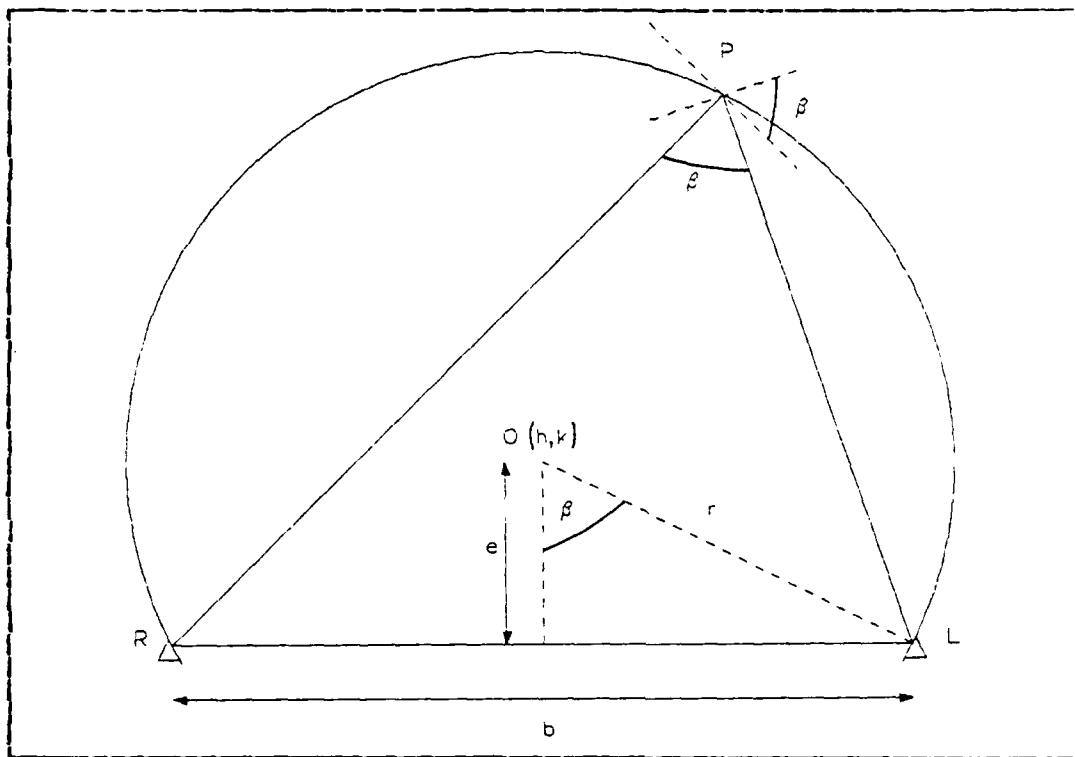


Figure 4.3 Construction of a Reliability Curve

LAB and MUSSEL for a range-range system ($\sigma_1 = \sigma_2 = 3$ meters) were constructed (Fig. 4.4). Using Equation 4.2, X-Y coordinates were generated for points laying on different reliability circles. A curve-fitting subroutine in the DISSPIA library was used to generate the circles through the computed points. The 13-meter accuracy contour corresponds to an angle of intersection of 31.6° , while the 7-meter accuracy contour corresponds to an angle of intersection of 67.9° . The best achievable accuracy of the system is 6.4 meters at 90° .

For comparison purposes, reliability contours were constructed about BEACH LAB and MUSSEL for azimuth-azimuth geometry ($\sigma_1 = \sigma_2 = 1.3$ meters). The increased accuracy of this configuration is evident (Fig. 4.5). The 3-meter

contour corresponds to an angle of intersection of 69.4° while the 6-meter contour corresponds to an angle of intersection of 29.6° . The best achievable accuracy at an intersection angle of 90° is 2.8 meters.

A second scheme was used to display accuracy predictions for the two positioning methods. Given the coordinates of EACH LAB and MUSSEL, a series of discrete points spaced 800 meters apart, were generated throughout the survey area. The values for the radii of 90 percent confidence circles were then computed at each point with the use of subroutine FROB. Figures 4.6 and 4.7 illustrate this prediction scheme. These figures present the same information as Figures 4.4 and 4.5 in a different manner. The 30° angle of intersection contour is shown on both figures.

GENERATED RELIABILITY CONTOURS

RANGE-RANGE: BEACH LAB-MUSSEL

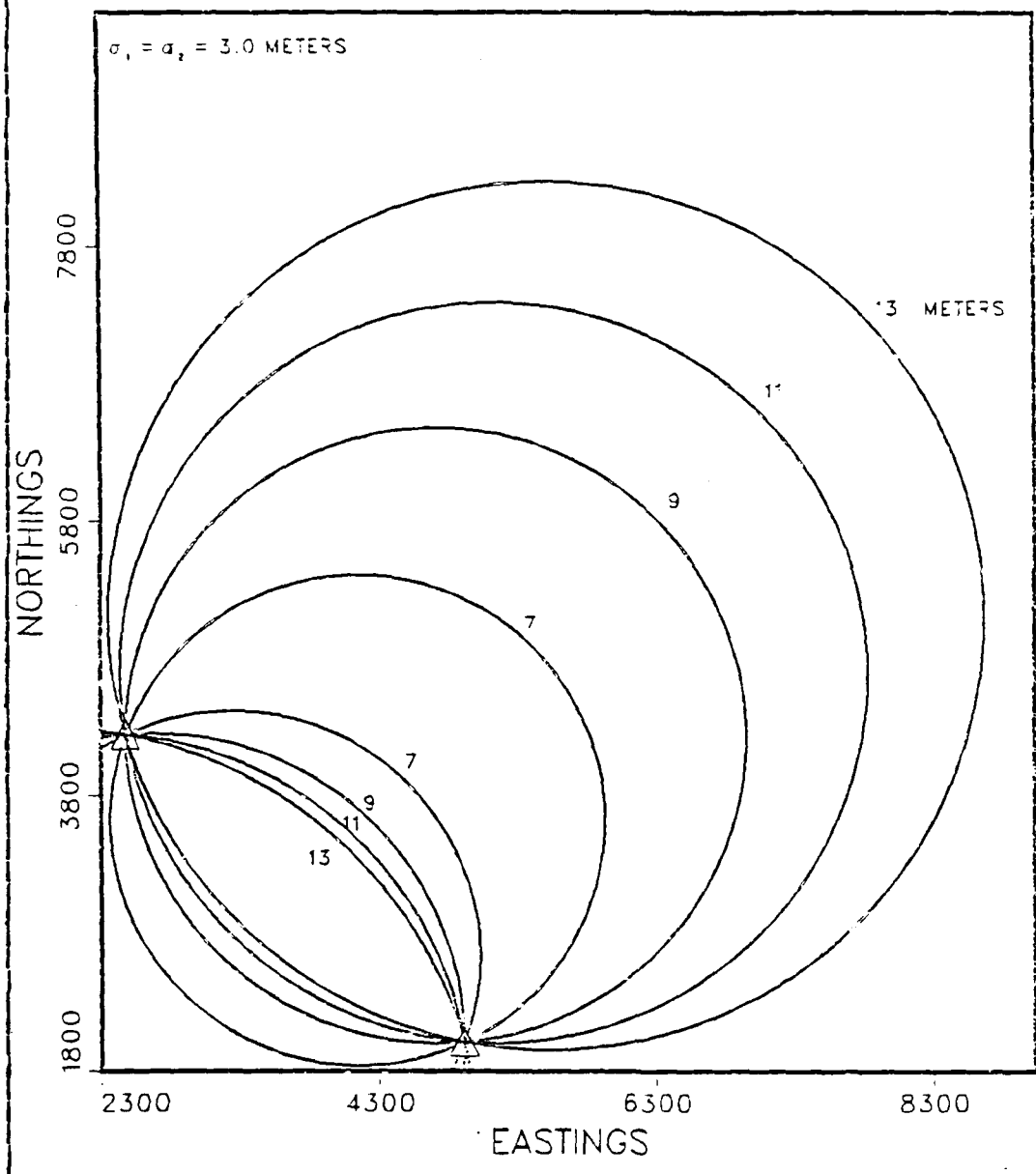


Figure 4.4 Reliability Contours: Range-Range Geometry

GENERATED RELIABILITY CONTOURS

AZIMUTH-AZIMUTH: BEACH LAB-MUSSEL

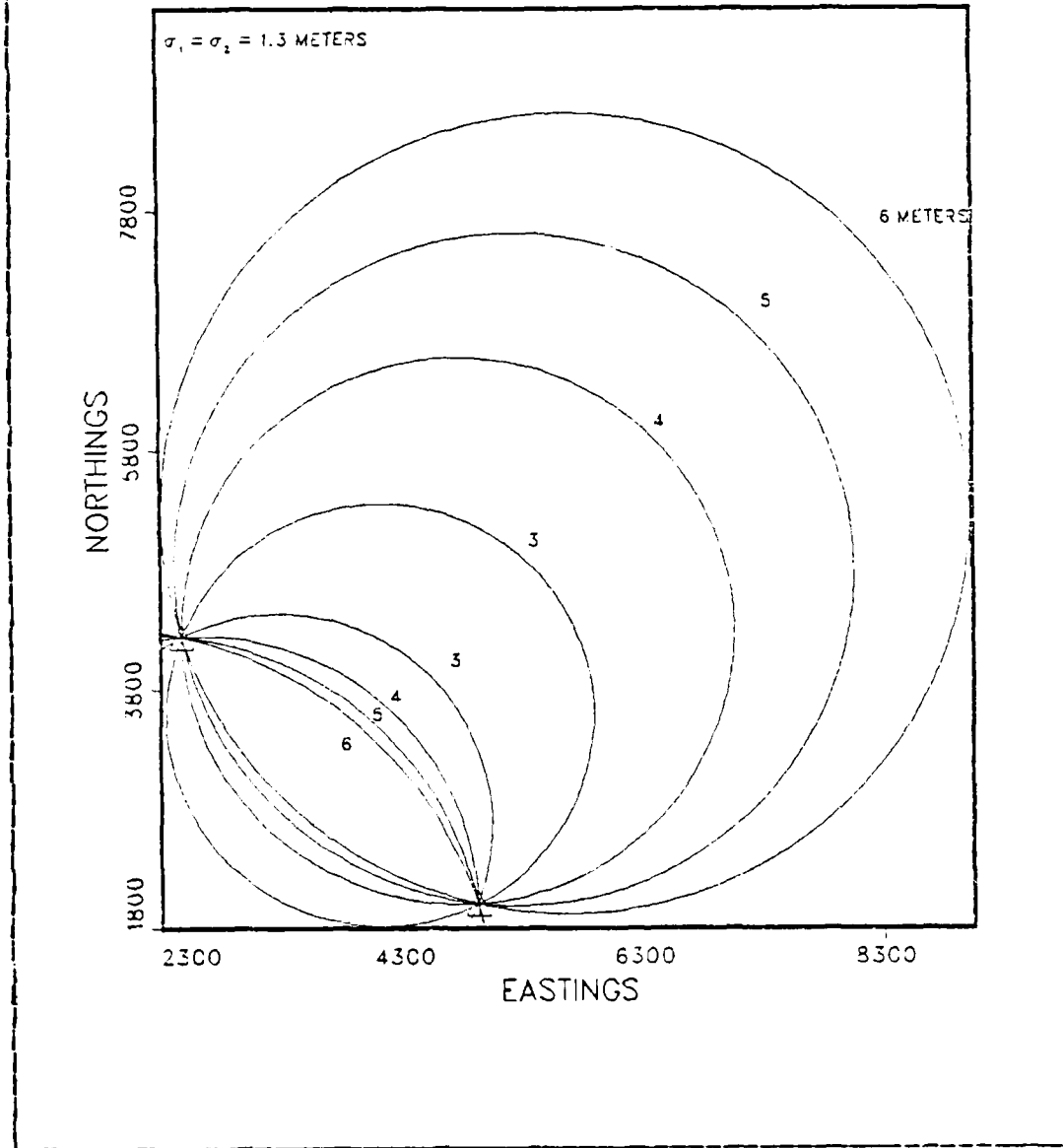


Figure 4.5 Reliability Contours: Azimuth-Azimuth Geometry

ACCURACY PREDICTIONS RA-RA
 RADII OF 90% PROBABILITY CIRCLES
 STATIONS BEACH LAB AND MUSSEL

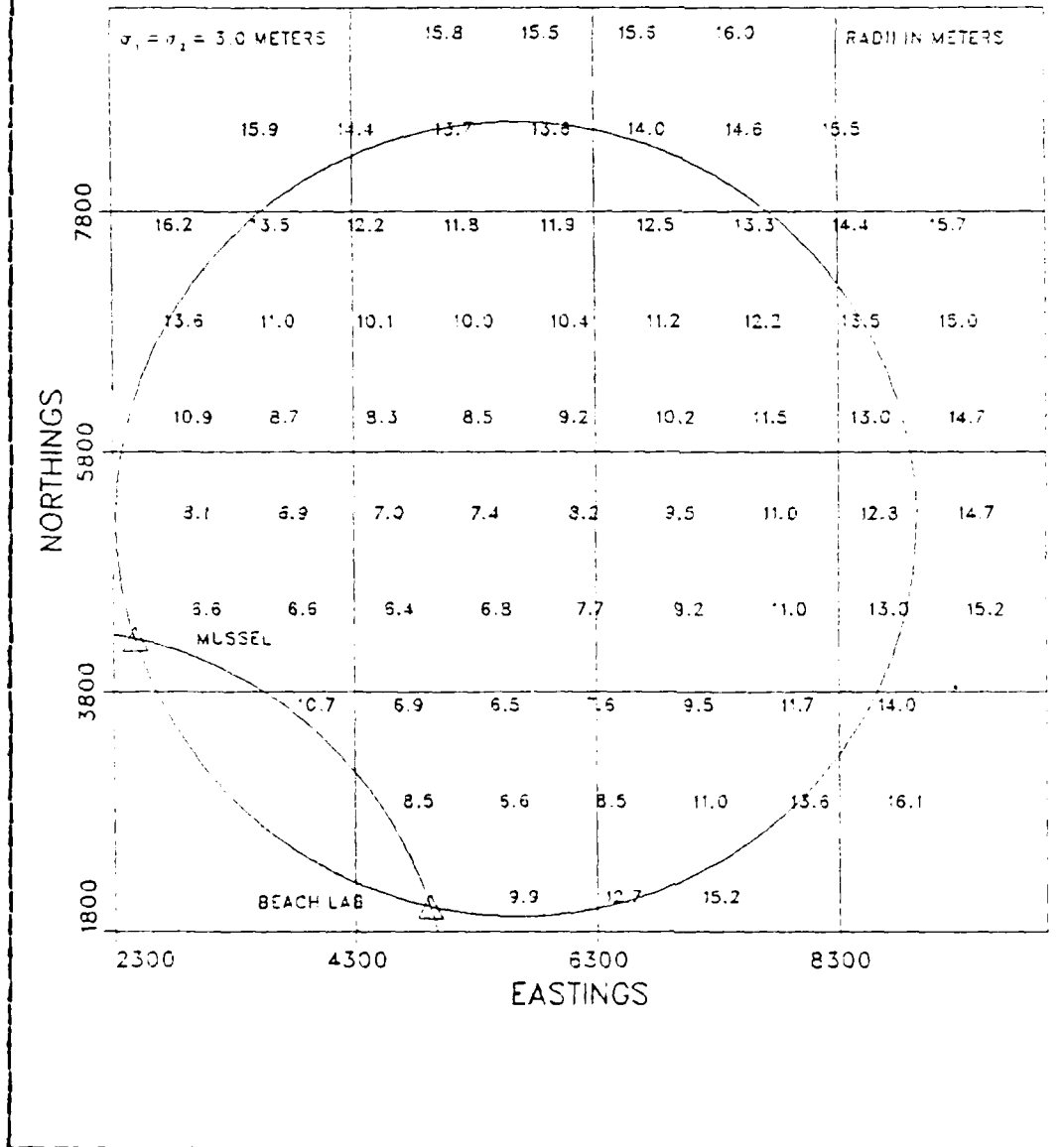


Figure 4.6 Range-Range Point Accuracy Prediction

ACCURACY PREDICTIONS AZ-AZ
 RADII OF 90% PROBABILITY CIRCLES
 STATIONS BEACH LAB AND MUSSEL

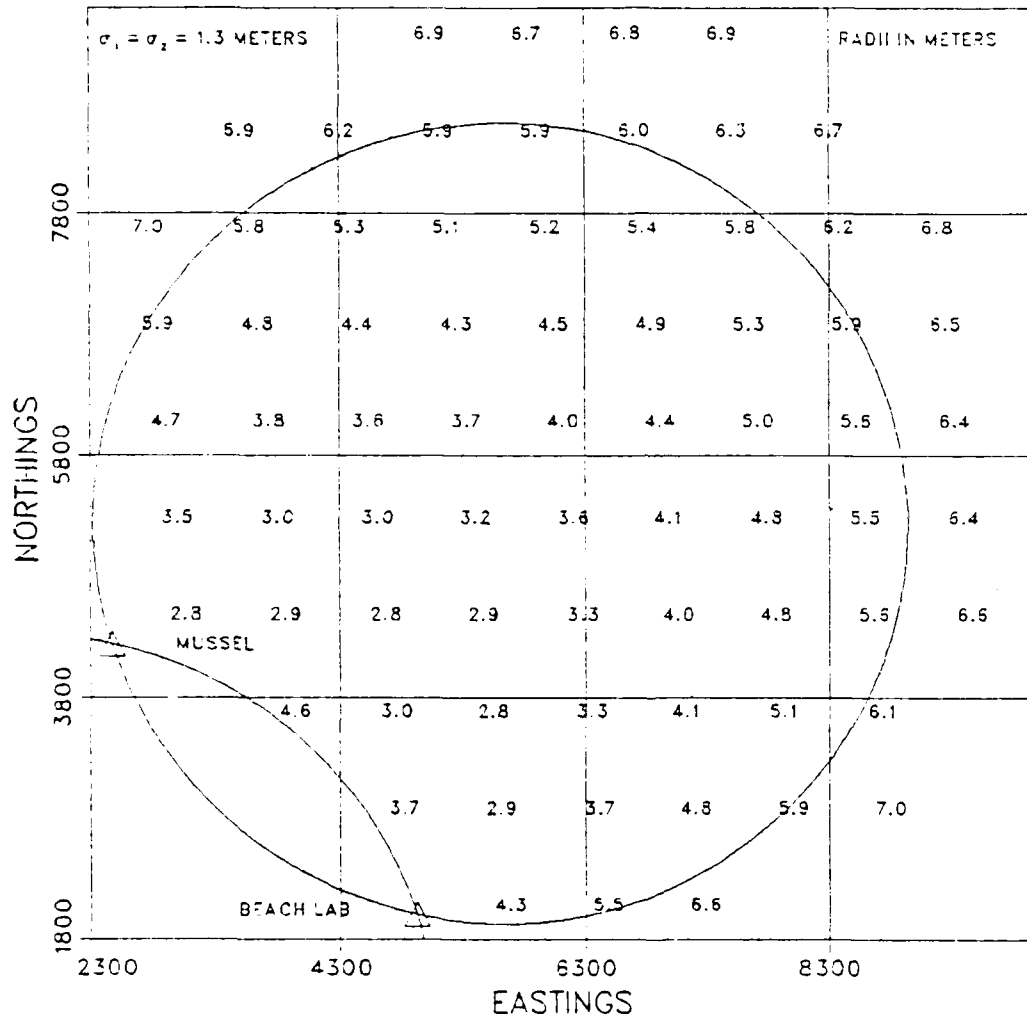


Figure 4.7 Azimuth-Azimuth Point Accuracy Prediction

V. CONCLUSIONS AND RECOMMENDATIONS

A. ACCURACY SPECIFICATIONS

Interpretation of the 1982 IHO positioning standards in terms of 90 percent confidence circles yields some interesting results with respect to present day survey practices. For example, for a 1:10,000-scale hydrographic survey, NOS usually uses microwave positioning systems in a range-range mode, and assumes a standard error of 3 meters for each LCP. Surveys are frequently conducted between the 30° to 150° angle of intersection limits. Using the 90 percent confidence circle criterion, the radius of the circle should not exceed 10 meters. However, the radius value for $\beta = 30^\circ$ and 150° is 13.7 meters. The values of $K\sigma_x$ and $K\sigma_y$ for the 90 percent confidence ellipse are 17.6 and 4.7 meters, respectively. To meet the 90 percent criterion for a 1:10,000-scale survey, the β limits should be 42° to 138°.

Azimuth-azimuth positioning is accurate enough for 1:5,000-scale surveys, using β limits of 35° to 145°, assuming a standard error of 1.3 meters for each LCP. With the standard error assumptions used for range-azimuth, the 90 percent radius is 5.1 meters for all positions. Given the uncertainties of the standard error figures, it is rational to assume that range-azimuth positions can meet the 5-meter accuracy standard for 1:5,000-scale surveys. In fact, range-azimuth positional accuracy can exceed azimuth-azimuth accuracy when the latter's β is less than 35°. For a 3-meter σ range-range configuration, it is impossible to meet 1:5,000 specifications with any β .

As a general guideline, the 30° to 150° angle of intersection limit is a good rule to use for uncorrelated LCP's.

CLASSIFIED AZIMUTH-AZIMUTH POSITIONS

Control Stations: USE MON 1978 and MUSSEL 1932

Standard Error Used in Computations: 1.3 meters

<u>Fix No.</u>	<u>X Coordinate</u>	<u>Y Coordinate</u>	<u>Angle of Intersection</u>	<u>Radius of 90° circle</u>
619	4449.26	2711.40	156.9	7.6
620	4437.86	2807.29	153.0	6.5
621	4427.41	2897.17	149.6	5.9
622	4419.65	2989.36	146.2	5.3
623	4410.42	3072.20	143.4	4.9
624	4390.60	3154.04	141.3	4.7
625	4376.52	3234.24	138.9	4.4
626	4364.31	3319.82	136.2	4.2
627	4348.71	3411.24	133.5	4.0
628	4334.31	3502.51	130.7	3.8
631	4333.97	3381.55	135.1	4.1
632	4333.79	3290.68	138.7	4.4
633	4327.70	3199.92	142.8	4.8
634	4322.53	3107.83	146.9	5.4
635	4323.18	3012.49	151.0	6.1
636	4322.44	2916.00	155.3	7.1
637	4327.25	2818.39	159.8	8.7
638	4339.77	2806.86	156.0	7.3
639	4386.58	2903.09	152.0	6.3
640	4377.29	2998.63	148.4	5.6
641	4367.00	3090.26	145.1	5.1
642	4355.55	3187.06	141.9	4.7
643	4345.97	3285.88	138.5	4.4
644	4256.90	3516.02	133.6	4.0
645	4260.68	3416.65	137.4	4.3
646	4264.77	3321.01	141.1	4.7
647	4283.59	3208.82	144.8	5.1
648	4303.24	3127.36	147.7	5.5
649	4300.30	3024.70	151.8	6.0
650	4345.53	3145.58	144.1	5.1
651	4370.38	3236.09	139.1	4.5
652	4398.77	3327.77	134.4	4.0
653	4411.48	3421.46	130.2	3.8
654	4438.30	3506.23	125.9	3.5
655	4470.97	3591.21	121.6	3.3
656	4502.73	3677.50	117.4	3.2
657	4514.38	3767.26	114.0	3.1
658	4512.00	3860.13	111.1	3.0
659	4520.10	3948.53	107.9	2.9
660	4494.79	3049.75	139.2	4.5
661	4487.96	3144.60	136.2	4.2
662	4477.62	3243.86	133.2	4.0
663	4462.90	3372.74	129.4	3.7
664	4453.74	3469.99	126.5	3.5
665	4440.56	3564.89	123.8	3.4
666	4465.02	3652.95	119.7	3.3
667	4507.24	3743.29	115.0	3.1
668	4577.55	3595.27	116.9	3.2
669	4569.50	3681.02	114.6	3.1
670	4563.68	3776.77	111.9	3.0
671	4564.53	3872.77	108.8	3.0
672	4563.90	3965.68	106.6	2.9
673	4560.41	4057.10	103.2	2.9
674	4553.49	4147.06	100.6	2.8
675	4556.71	4239.64	97.7	2.8
677	4571.60	4416.22	92.0	2.8
678	4576.20	4504.92	89.3	2.8
679	4582.23	4597.03	86.5	2.8
680	4604.35	4631.33	85.1	2.8
681	4613.39	4527.17	87.9	2.8

RANGE-RANGE ACCURACIES (CONTINUED)

<u>Fix No.</u>	<u>X Coordinate</u>	<u>Y Coordinate</u>	<u>Angle of Intersection</u>	<u>Radius of 90% circle</u>
806	3830.54	4843.53	92.8	6.4
807	3877.77	4734.18	88.3	6.4
808	3907.61	4618.18	83.4	6.5
809	3932.77	4495.95	78.1	6.6
810	3948.19	4376.06	72.8	6.8
811	3956.79	4251.77	67.0	7.0
812	3953.81	4125.89	60.9	7.5
813	3938.32	3995.79	54.1	8.1
814	3909.94	3869.78	46.9	9.1
815	3864.71	3744.84	38.9	10.7
816	3816.98	3619.07	30.6	13.4
817	3711.62	5131.00	104.5	6.7
818	3788.16	5014.61	99.7	6.5
819	3851.30	4889.79	94.7	6.5
820	3901.13	4761.08	89.6	6.4
821	3961.73	4590.52	82.7	6.5
822	3977.10	4485.23	78.2	6.6
823	3993.32	4118.31	61.5	7.4
824	3996.85	4193.81	65.2	7.2
825	3981.72	4048.49	57.9	7.7
826	3956.88	3905.60	50.2	8.6
827	3916.26	3758.91	41.5	10.1
828	3826.04	3553.55	27.6	14.8
829	3961.88	4691.61	87.1	6.4
830	3907.91	4827.37	92.4	6.4
831	3841.30	4953.23	97.3	6.5
832	3789.42	5085.46	102.4	6.6
833	3772.12	5177.05	105.8	6.7
834	3843.76	5069.86	101.7	6.6
835	3906.65	4961.46	97.6	6.5
836	3959.36	4844.18	93.3	6.4
837	4002.25	4720.39	88.6	6.4
838	4057.98	4659.81	86.7	6.4
839	3992.26	4828.76	92.8	6.4
840	3954.08	4915.16	96.0	6.5
841	3905.75	5046.63	100.8	6.6
842	3822.81	5167.39	105.2	6.7
843	3844.43	5129.36	103.8	6.6
844	3958.55	5033.27	100.3	6.6
845	4016.73	4919.44	96.4	6.5
846	4061.27	4797.13	92.1	6.4
847	4159.72	4597.99	85.5	6.5
848	4119.01	4735.07	90.2	6.4
849	4077.07	4872.84	95.0	6.5
850	4021.39	4990.89	99.0	6.5
851	3961.68	5118.03	103.3	6.6
852	3992.88	5139.94	104.0	6.6
853	4056.51	5026.15	100.3	6.7
854	4121.60	4874.08	95.4	6.5
855	4154.57	4779.44	92.2	6.4
856	4196.42	4617.75	86.7	6.4

RANGE-RANGE ACCURACIES (CONTINUED)

Fix No.	X Coordinate	Y Coordinate	Angle of Intersection	Radius of 90% Circle
742	3570.50	4836.50	92.8	6.4
743	3618.79	4723.26	87.0	6.4
744	3662.90	4602.44	80.9	6.5
745	3691.10	4478.20	74.4	6.7
746	3715.24	4341.39	67.1	7.0
747	3720.11	4205.94	59.5	7.6
748	3703.21	4071.17	51.4	8.5
749	3678.03	3939.55	43.0	9.8
750	3636.04	3801.29	33.7	12.3
751	3630.00	3715.02	28.3	14.5
752	3678.77	3812.88	35.7	11.6
753	3715.73	3925.96	43.4	9.7
754	3731.48	4050.62	51.0	8.5
755	3756.38	4168.71	58.3	7.7
756	3754.68	4300.89	65.5	7.1
757	3743.02	4427.92	72.2	6.8
758	3710.29	4554.17	78.6	6.6
759	3680.62	4673.88	84.6	6.5
760	3627.42	4792.51	90.5	6.4
761	3572.80	4899.46	95.8	6.5
762	3627.15	4891.25	95.1	6.5
763	3683.33	4778.34	89.7	6.4
764	3725.77	4656.01	83.9	6.5
765	3757.98	4525.66	77.5	6.6
766	3781.56	4403.13	71.5	6.8
767	3798.56	4272.52	64.8	7.2
768	3787.95	4134.55	57.1	7.8
769	3772.73	4001.69	49.4	8.7
770	3738.73	3870.33	41.1	10.2
771	3695.62	3745.45	32.6	12.7
772	3712.52	3708.43	31.2	13.2
773	3777.45	3829.70	40.2	10.4
774	3803.43	3957.03	48.0	9.0
775	3818.28	4087.24	55.4	8.0
776	3831.33	4211.74	62.3	7.4
777	3823.70	4338.97	68.8	6.9
778	3813.41	4476.12	75.6	6.7
779	3777.13	4614.24	82.1	6.5
780	3739.58	4736.39	87.8	6.4
781	3691.63	4868.16	93.9	6.5
782	3706.65	4918.98	96.0	6.5
783	3749.46	4806.82	91.1	6.4
784	3799.89	4705.41	86.6	6.4
785	3829.30	4581.14	81.0	6.5
786	3857.30	4455.00	75.1	6.7
787	3868.49	4327.66	69.0	7.0
788	3872.94	4198.56	62.5	7.3
789	3862.59	4062.95	55.3	8.0
790	3841.17	3922.97	47.7	9.0
791	3804.62	3797.14	39.4	10.6
792	3759.45	3596.86	27.1	15.1
793	3808.16	3722.44	35.6	11.6
794	3851.17	3827.55	42.7	9.9
795	3879.16	3942.93	49.6	8.7
796	3896.63	4068.89	56.5	7.9
797	3903.40	4184.15	62.5	7.3
798	3916.60	4306.31	68.8	6.9
799	3904.40	4428.30	74.5	6.7
800	3879.66	4554.38	80.2	6.5
801	3851.19	4684.13	85.9	6.5
802	3810.16	4796.95	90.7	6.4
803	3752.88	4908.69	95.5	6.5
804	3706.66	4998.99	99.4	6.5
805	3781.90	4945.89	97.0	6.5

RANGE-RANGE ACCURACIES (CONTINUED)

Fix No.	X Coordinate	Y Coordinate	Angle of Intersection	Radius of 90° Circle
120	3261.07	4111.17	42.0	10.0
121	3262.51	4368.76	63.7	7.3
122	3175.94	4613.63	83.8	6.5
123	3189.26	4667.90	87.5	6.4
124	3228.57	4471.03	71.9	6.8
125	317.76	4240.01	53.9	8.1
126	3228.62	4020.86	35.3	11.7
127	3222.48	3951.93	28.6	14.3
128	3300.99	3962.87	31.8	13.0
129	3333.57	4200.72	51.7	8.4
130	3331.06	4454.74	70.7	6.9
131	3228.99	4654.02	85.4	6.5
132	3228.69	4673.74	86.3	6.5
133	3266.26	4474.82	72.2	6.8
134	3388.38	4275.01	57.7	7.8
135	3376.70	4076.27	42.6	9.9
136	3337.33	3910.52	29.0	14.1
137	3345.86	3873.34	26.7	15.3
138	4422.73	4077.78	44.0	9.6
139	331.43	4314.80	61.3	7.4
140	3396.21	4530.82	76.0	6.6
141	3262.96	4700.26	87.4	6.4
142	331.30	4694.84	86.7	6.4
143	3366.64	4506.04	74.4	6.7
144	3474.89	4309.23	61.5	7.4
145	3464.73	4120.80	48.2	8.9
146	3425.35	3933.68	34.0	12.2
147	3419.34	3928.23	34.8	11.9
148	3413.95	4137.04	50.6	8.5
149	3412.94	4390.84	67.4	7.0
150	3473.67	4567.85	78.4	6.6
151	3388.01	4766.90	90.7	6.4
152	3350.09	4801.65	92.5	6.4
153	3472.78	4657.67	83.8	6.5
154	3427.62	4492.63	73.9	6.7
155	3455.04	4377.14	67.0	7.1
156	3411.04	4288.00	61.4	7.4
157	3433.95	4204.99	55.7	7.9
158	3433.69	4262.39	59.5	7.6
159	3433.85	4068.09	46.8	9.1
160	3493.62	3880.18	32.9	12.5
719	3419.28	3843.16	31.6	13.0
720	3458.31	4061.28	47.6	9.0
721	3489.75	4237.59	58.7	7.7
722	3488.78	4441.75	71.1	6.8
723	3425.50	4623.58	81.7	6.5
724	3442.67	4796.98	91.7	6.4
725	3478.48	4818.98	92.6	6.4
726	3455.35	4658.77	83.7	6.5
727	3412.48	4473.89	73.4	6.7
728	3435.37	4279.04	62.1	7.4
729	3418.98	4069.08	49.0	8.8
730	3457.84	3866.91	35.1	11.8
731	3487.72	3809.47	32.1	12.8
732	3413.95	3910.30	39.1	10.7
733	3464.48	4007.29	46.1	9.3
734	3476.20	4121.41	53.6	8.2
735	3477.60	4225.91	59.8	7.6
736	3476.79	4332.54	66.0	7.1
737	3458.87	4436.08	71.7	6.8
738	3438.19	4545.66	77.6	6.6
739	3404.38	4649.50	83.2	6.5
740	3457.48	4754.18	88.7	6.4
741	3414.26	4836.98	93.2	6.4

RANGE-RANGE ACCURACIES (CONTINUED)

Fix No.	X Coordinate	Y Coordinate	Angle of Intersection	Radius of 90% Circle
51	3114.26	4776.58	96.5	6.5
52	3921.85	4647.63	94.8	6.5
53	3753.76	4502.52	91.5	6.4
54	3793.31	4487.76	86.6	6.4
55	360.81	4619.38	90.6	6.4
56	3160.14	4750.25	93.6	6.4
57	3225.11	4847.99	96.0	6.5
58	3492.32	4942.05	98.4	6.5
59	3693.83	5032.60	100.8	6.5
61	3668.42	4910.65	96.3	6.5
62	3370.43	4812.54	93.4	6.4
64	3174.72	4695.41	89.7	6.4
65	3998.35	4566.29	84.5	6.5
66	3824.36	4433.37	76.9	5.6
67	3819.19	4368.35	67.7	7.0
68	33002.82	4519.53	80.0	6.5
69	3184.74	4657.79	86.9	6.4
70	3378.02	4763.00	90.5	6.4
71	3578.71	4871.32	94.4	6.5
72	3788.85	4962.48	97.7	6.5
73	4010.25	5031.39	100.4	6.6
74	3732.84	4895.17	95.5	6.5
75	3509.99	4799.08	91.3	6.4
76	3307.18	4688.48	86.9	6.4
77	3094.50	4546.29	80.1	6.5
78	3091.06	4391.68	68.5	7.0
79	3754.33	4263.59	49.5	8.7
80	3754.15	5020.93	100.1	6.5
81	3514.53	4919.46	97.2	6.5
82	3287.25	4788.27	93.3	6.4
84	3062.52	4651.12	89.4	6.4
84	3846.46	4482.96	82.4	6.5
84	3845.13	4562.17	91.3	6.4
85	3995.88	4403.69	68.0	7.0
86	3165.76	4254.99	52.7	8.8
87	331.61	4102.46	43.3	9.8
88	3500.54	3946.44	37.5	11.1
89	3672.90	3785.70	34.0	12.2
90	3846.42	3623.19	32.0	12.9
91	4022.93	3464.18	31.6	13.0
92	4406.76	3998.00	68.3	7.0
93	4263.63	4159.42	70.3	6.9
94	4112.66	4331.20	73.9	6.7
95	3959.57	4527.77	79.9	6.5
96	410.03	4681.47	85.5	6.5
97	3672.32	4864.18	93.7	6.5
98	335.90	5040.98	102.3	6.6
100	365.44	4352.97	61.8	7.4
101	3068.28	4166.32	41.6	10.1
102	3077.08	4046.24	29.5	13.9
103	3117.61	4262.88	52.8	8.3
104	3062.15	4499.11	76.5	6.6
105	3011.82	4658.04	91.7	6.4
106	3122.91	4453.24	71.4	6.8
107	3152.10	4199.54	47.1	9.1
108	3118.73	4025.84	29.3	14.0
110	3188.79	4154.61	43.8	9.7
111	3177.20	4396.30	65.9	7.1
112	311.79	4583.07	82.8	6.5
113	3182.67	4534.87	77.6	6.6
114	3099.29	4691.03	91.3	6.4
115	3209.60	4484.20	73.3	6.7
116	335.42	4271.54	55.2	8.0
117	2204.85	4043.52	34.3	12.0

APPENDIX B

ACCURACY CLASSIFICATION: 90 PERCENT CONFIDENCE CIRCLES

CLASSIFIED RANGE-RANGE POSITIONS

Control Stations: BEACH LAB 1982 and MUSSEL 1932

Standard Error Used in Computations: 3 meters

<u>Fix No.</u>	<u>X Cordinate</u>	<u>Y Cordinate</u>	<u>Angle of Intersection</u>	<u>Radius of 90% Circle</u>
1	2668.05	4942.07	127.0	8.2
2	2852.01	5076.69	121.6	7.7
3	3041.58	5194.85	118.6	7.4
4	3040.27	5148.74	117.0	7.3
5	2838.26	5021.35	120.2	7.6
6	2640.06	4877.13	126.9	8.2
7	2553.46	4752.36	130.4	8.7
8	2724.10	4885.47	121.3	7.7
9	2889.06	5013.63	117.6	7.3
10	3075.61	5124.37	115.0	7.2
11	3172.63	5136.23	112.7	7.0
12	2958.13	5006.65	114.4	7.1
13	2771.33	4876.02	117.9	7.4
14	2581.02	4729.89	126.9	8.2
15	2584.41	4665.31	124.0	7.9
16	2740.05	4805.63	116.7	7.3
17	2913.27	4928.51	112.8	7.0
18	3097.44	5047.77	111.2	6.9
19	3193.94	5103.46	110.9	6.9
20	2627.47	4659.05	118.8	7.4
21	2762.15	4769.60	113.2	7.1
22	2904.91	4875.24	110.5	6.9
23	3056.38	4975.73	109.3	6.9
24	3207.36	5064.00	108.9	6.8
25	3373.36	5101.96	107.1	6.8
26	3190.64	5007.38	106.8	6.8
27	3015.45	4900.75	107.1	6.8
28	2839.38	4778.31	108.7	6.8
29	2679.99	4651.31	112.8	7.0
30	2727.88	4632.77	106.9	6.8
31	2899.83	4776.97	105.2	6.7
32	3092.77	4901.75	104.4	6.6
33	3295.42	5019.92	105.0	6.7
34	3502.07	5123.36	106.0	6.7
35	3697.02	5151.09	105.3	6.7
36	3474.77	5065.57	104.0	6.7
37	3257.48	4953.37	102.7	6.6
38	3043.03	4821.88	101.7	6.6
39	2845.07	4680.80	101.7	6.6
40	2746.96	4608.32	103.1	6.6
41	2748.09	4550.40	97.5	6.5
42	2931.78	4701.21	98.4	6.5
43	3134.33	4834.56	99.4	6.5
44	3317.94	4944.55	101.0	6.6
45	3515.14	5043.56	102.6	6.6
46	3720.18	5117.15	103.9	6.6
48	3724.93	5083.62	102.6	6.6
49	3514.33	4989.13	100.3	6.6
50	3312.88	4891.55	98.5	6.5

```

ELSE IF (C.GE.0.6).AND.(C.GT.0.5)) THEN
  B=0.7101*C+1.36546
  B=C.444*C+1.46488
ELSE IF ((C.GE.0.5).AND.(C.GT.0.4)) THEN
  B=C.3790*C+1.54758
ELSE IF ((C.GE.0.4).AND.(C.GT.0.3)) THEN
  B=0.2535*C+ 1.59778
ELSE IF ((C.GE.0.3).AND.(C.GT.0.2)) THEN
  B=0.1652*C+1.62427
ELSE IF ((C.GE.0.2).AND.(C.GT.0.1)) THEN
  B=.094*C+1.63851
ELSE
  B=0.0306*C+1.64485
END IF
RADIUS=B*SIGX
SGX90=2.146*SIGX
SGY90=2.146*SIGY
CIRAR=3.1415926*RADIUS**2
ELAR=3.1415926*SGX90*SGY90
RETURN
END

```

APPENDIX A

SUBROUTINE FOR 90 PERCENT CONFIDENCE CIRCLE PARAMETERS

```

SUBROUTINE PROE (SIG1, SIG2, COR, TBETA, SGX90, SGY90,
* RADIUS, ELAR, CIRAR)
IMPLICIT REAL*4 (A-H, O-Z)
C COMPUTES RADIUS OF 90% CONFIDENCE CIRCLE (BURT, METHOD 2)
C THIS SUBROUTINE WORKS FOR CORRELATED AND UNCORRELATED
C LINES OF POSITION.
C
C INPUT PARAMETERS:
C   SIG1 AND SIG2- STANDARD ERRORS OF TWO LOP'S
C   TBETA        - ANGLE OF INTERSECTION IN DEGREES
C                 (0-180 DEG)
C   COR         - CORRELATION COEFFICIENT
C                 (USUALLY ZERO EXCEPT FOR HYPERBOLIC
C                 OR SEXTANT POSITIONING)
C
C OUTPUT PARAMETERS:
C   SGX90 AND SGY90- SEMI-MAJOR AND MINOR AXES
C                   OF 90% ERROR ELLIPSE
C   RADIUS        - RADIUS OF 90% CONFIDENCE CIRCLE
C   ELAR         - AREA OF 90% CONFIDENCE ELLIPSE
C   CIRAR        - AREA OF 90% CONFIDENCE CIRCLE
C
C WORK WITH AN ANGLE LESS THAN 90 DEGREES
C   IF (TBETA .GT. 90.) BETA = 180.-TBETA
C   IF (TBETA .LE. 90.) BETA = TBETA
C CHANGE DEGREES TO RADIANS
C   RAL = .0174532 * BETA
C TRANSFORMATION SIG1 AND SIG2 TO CORRELATED
C RECTANGULAR SYSTEM
C   SIGA = SQRT ((1. / (1 + (SIN (RAD) ** 2)) * (SIG1 ** 2 + 2. * COR * SIG1 *
* SIG2 * COS (RAD) + SIG2 ** 2) - SIG2 ** 2))
C   SIGB = SIG2
C TRANSFORM CORRELATION COEFFICIENT TO CORRELATED
C RECTANGULAR COORDINATE SYSTEM
C   A = ((SIG2 * COS (RAL)) / SIG1) + COR
C   F = 1 / SQRT (1 + 2 * COR * SIG2 * COS (RAD) / SIG1 + (SIG2 / SIG1) ** 2 *
* (COS (RAD) ** 2))
C   CORAB = A * F
C TRANSFORM TO UNCORRELATED RECTANGULAR
C   AA = SQRT ((SIGA ** 2 + SIGB ** 2) / 2)
C   CC = SQRT (1 - (4 * SIGA ** 2 * SIGB ** 2 * (1 - CORAB ** 2)) /
* (SIGA ** 2 + SIGB ** 2) ** 2)
C   DD = SQRT (1 + CC)
C   SIGX = AA * DD
C   SIGY = SQRT (SIGA ** 2 + SIGB ** 2 - SIGX ** 2)
C
C COMPUTE ECCENTRICITY OF ELLIPSE
C   C = SIGY / SIGX
C COMPUTE BURT'S K FACTOR BY LINEAR INTERPOLATION
C   IF ((C .LE. 1.) .AND. (C .GT. 0.9)) THEN
C     B = 1.0361 * C + 1.10987
C   ELSE IF ((C .LE. 0.9) .AND. (C .GT. 0.8)) THEN
C     B = 0.9475 * C + 1.18961
C   ELSE IF ((C .LE. 0.8) .AND. (C .GT. 0.7)) THEN
C     B = 0.8508 * C + 1.26697
C   ELSE IF ((C .LE. 0.7) .AND. (C .GT. 0.6)) THEN

```

Many variables exist when considering accuracy requirements for a hydrographic survey. In general, higher accuracy means more time, money, and effort. Azimuth-azimuth geometry is the most accurate method of positioning analyzed in this thesis. This method involves at least two people ashore and good ship-to-shore communications. Currently, NOS acquires these data manually, which minimizes the speed that the vessel can operate and adds to processing time. On the other hand, a survey using a medium-range system needs little shore support and the data acquisition is automated. Accuracy predictions help keep a balance between accuracy and effort. If the desired accuracy is attainable using a range-range system instead of an azimuth-azimuth system, then the choice is obvious.

Hydrographic positioning in the future will be dominated by two methods. For offshore surveys, the Global Positioning System (GPS) is expected to give positional accuracy to 10 meters or better. GPS is a satellite positioning system currently being deployed by the Department of Defense and will provide near worldwide coverage for users. Since the full constellation of 18 satellites will not be operational until 1988, it is not yet known if the expected accuracy of 10 meters will be met. Nearshore surveys may use multiple LOP's for establishing hydrographic positions. The principle of least squares is applied to redundant observations yielding the most probable position. For both GPS and least squares positioning, confidence ellipses and circles can be determined, although the techniques involved are much more complicated than those presented in this thesis.

The accuracy classification scheme presented in this thesis is predicated on the elimination of systematic errors. Much work is needed in identifying the sources of systematic errors associated with hydrographic positioning equipment.

lengthened. In an investigation such as this, it is advisable to be conservative and use the maximum length of line which is operationally feasible to provide coverage of an area as large as possible. The radius of the 90 percent confidence circle gives the hydrographer a rough figure for answering the question: Does the submerged pile exist?

Knowing the parameters of the error ellipse could be useful for conducting wire-drag, wire-sweep, and side scan sonar operations. For a position obtained with low precision positioning equipment, the search to relocate a submerged feature could cover a large area. Knowing the parameters of the error ellipse could reduce the area, time, and effort of the search. The search pattern could be planned to cover the desired confidence ellipse.

With the quantification of accuracy, a decision must be made concerning how much confidence is needed to delete a certain feature from the chart after a search has been made. The 90 percent confidence level may be too low, whereas the 95 or 99 percent level may suffice. A balance must be maintained between confidence of disproof and time and effort spent on the search.

Accuracy predictions in the form of reliability contours can be displayed using computer graphic terminals. These displays will contribute to the efficient planning of surveys to meet specifications. Given the survey area, the available control, the positioning methods, and the precision of the positioning equipment, the hydrographer can plan the accuracy of the survey before it is conducted. The survey area and the available control may be such that there is flexibility to change control stations to optimize accuracy over an area of critical importance. This information can be displayed graphically and plans for the survey can be made accordingly. Likewise, given an accuracy limit, such as a 10-meter radius of the 90 percent confidence circle, the area to be covered at that accuracy can be maximized.

B. USES FOR ACCURACY FIGURES

NCS is currently developing the Shipboard Data System III (SDS III), a hydrographic data acquisition and processing system which will replace the present HYDROLOG/HYDROFLOT system. SDS III will revolutionize data acquisition and processing techniques with the capability to perform high-speed calculations and display color graphics. With this increased computer potential, data manipulations--such as accuracy computations--can be performed.

Each position in a survey can be given a quality figure based on the radius of the 90 percent confidence circle. This figure is sufficient for non-critical positions of ordinary hydrographic data. Critical positions are those which are determined for significant features (i.e., wrecks, least depths, rocks, and other potential hazards). For these positions, the parameters of the 90 percent error ellipse can be computed, as well as the radius of the 90 percent confidence circle.

Many schemes can be envisioned for the use of an accuracy figure. For example, suppose the position of a submerged pile was determined by range-azimuth geometry in a prior survey. The radius of the 90 percent confidence circle is then 5.1 meters (Ex. 2, Ch. II). The charting agency now wishes to relocate the pile to determine if it still exists and is still a hazard to navigation. In low water visibility, a common technique used to resolve such an item would be to send divers down over the reported position and conduct a circle search. One diver remains at the reported position, holding a line, while the other diver swims a circumference holding the other end of the line. Theoretically, if the line is about 5 meters long and a hang does not occur, it is 90 percent certain that the pile has been removed. For a higher confidence, the line is

figures as a function of β for uncorrelated LCP's have been compiled using standard errors of 1.3 meters for azimuth-azimuth (Table VIII), 3.0 meters for range-range short-range (Table IX), and 10 meters for range-range medium-range (Table X) positioning systems.

TABLE VIII

Accuracy Figures for $\sigma_1 = \sigma_2 = 1.3 \text{ m}$, $\rho_{12} = 0$

Angle of Inter. (deg)	$K\sigma_x$ (m)	$K\sigma_y$ (m)	Radius of 90% Circ. (m)	Area of Ellipse (sq m)	Area of Circle (sq m)
90	2.8	2.8	2.8	24	24
85	2.9	2.7	2.8	25	25
80	3.1	2.6	2.8	25	25
75	3.2	2.5	2.9	25	26
70	3.4	2.4	3.0	26	28
65	3.7	2.4	3.1	27	30
60	3.9	2.3	3.3	28	34
55	4.7	2.3	3.5	30	38
50	5.1	2.2	3.8	32	44
45	5.1	2.1	4.1	35	53
40	5.8	2.1	4.5	38	65
35	6.6	2.1	5.1	43	83
30	7.6	2.0	5.9	49	110
25	9.1	2.0	7.1	58	156
20	11.4	2.0	8.8	71	241
15	15.1	2.0	11.6	94	425
10	22.6	2.0	17.4	141	949
5	45.2	2.0	34.7	281	3,781

$K = 2.146$ for 90% probability

However, as mentioned for 1:10,000-scale surveys in a range-range mode ($\sigma = 3$ meters), this rule does not always hold. On the other hand, it is possible to have β 's of less than 30° and still meet specifications. For example, azimuth-azimuth positioning can theoretically be used for β 's of 180° to 162° for a 1:10,000-scale survey. However, the eccentricity of the error ellipse is so small that the distortion introduced by using confidence circles can become misleading. In view of this, eccentricities of less than 0.2 should not be used.

Using the 90 percent radius criterion, a table has been assembled illustrating the β limit for various positioning geometries at different survey scales, using assumed standard errors (Table VII). The information in Table VII illustrates that the 30° to 150° β limit need not be fixed. The β limits should vary based on the scale of the survey and the precision of the positioning equipment. Accuracy

TABLE VII
 β Limits for Surveys

Survey Scale	90% Radius (m)	R-R ($\sigma = 3$) β Limit (deg)	R-R ($\sigma = 10$) β Limit (deg)	Az-Az ($\sigma = 1.3$) β Limit (deg)
1:2,500	2.5	-----	-----	-----
1:5,000	5.0	-----	-----	35-145
1:10,000	10.0	42-138	-----	23-157*
1:20,000	20.0	27-153	-----	23-157*
1:40,000	40.0	23-157*	35-145	23-157*

* Eccentricity limit of 0.2

Note: 90% radii of all range-azimuth positions are assumed to be 5.1 meters for $\sigma_1 = 3$ and $\sigma_2 = 1.3$.

AZIMUTH-AZIMUTH ACCURACIES (CONTINUED)

<u>Fix No.</u>	<u>X Coordinate</u>	<u>Y Coordinate</u>	<u>Angle of Intersection</u>	<u>Radius of 90% Circle</u>
682	4611.20	4421.29	91.0	2.8
683	4610.07	4315.24	94.1	2.8
684	4609.84	4204.66	97.4	2.8
685	4603.99	4098.63	100.7	2.8
686	4600.52	3992.16	104.0	2.8
687	4601.27	3883.40	107.3	2.8
688	4601.13	3780.02	110.4	3.0
689	4602.22	3675.49	113.5	3.1
690	4601.48	3574.94	116.5	3.1
691	4603.21	3458.09	120.0	3.3
692	4524.84	3728.78	114.8	3.1
693	4657.06	3506.75	116.1	3.1
694	4648.60	3602.24	113.7	3.1
697	4630.15	3696.13	111.8	3.0
698	4629.80	3793.39	108.9	3.0
699	4623.03	3889.32	106.3	2.9
700	4622.83	3978.70	103.7	2.9
701	4617.60	4071.98	101.1	2.8
702	4623.30	4163.73	98.2	2.8
703	4618.23	4256.25	95.7	2.8

CLASSIFIED RANGE-AZIMUTH POSITIONS

Control Stations: MUSSEL 1932 occupied, initial USE MCN 1978

Standard Errors: Range--3 meters; T-2--1.3 meters

<u>Fix No.</u>	<u>X Coordinate</u>	<u>Y Coordinate</u>	<u>Angle of Intersection</u>	<u>Radius of 90% Circle</u>
414	2898.58	4611.99	90.0	5.1
415	2979.40	4483.31	90.0	5.1
416	3027.69	4342.47	90.0	5.1
417	2795.26	4216.04	90.0	5.1
418	3002.90	4061.15	90.0	5.1
419	2939.58	3938.67	90.0	5.1
420	2904.53	3888.38	90.0	5.1
421	3195.47	3388.00	90.0	5.1
422	3128.22	3487.82	90.0	5.1
423	3048.17	3599.79	90.0	5.1
424	2994.68	3723.65	90.0	5.1
425	2911.61	3833.20	90.0	5.1
426	2883.62	3921.16	90.0	5.1
427	2749.17	4000.71	90.0	5.1
428	2752.46	4029.48	90.0	5.1
429	2823.93	3969.92	90.0	5.1
430	2894.60	3920.66	90.0	5.1
431	2907.95	3839.53	90.0	5.1
432	2961.44	3901.64	90.0	5.1
433	3005.23	3980.11	90.0	5.1
434	3037.78	4058.01	90.0	5.1
435	3065.09	4134.51	90.0	5.1
436	3074.88	4036.74	90.0	5.1
437	3048.02	3953.93	90.0	5.1
438	2999.66	3871.95	90.0	5.1
439	2943.10	3809.76	90.0	5.1
440	1128.59	4049.87	90.0	5.1
441	0996.20	3997.78	90.0	5.1
442	0588.84	3897.24	90.0	5.1
443	0099.61	3825.86	90.0	5.1
444	14.71	3837.97	90.0	5.1
445	068.50	3755.28	90.0	5.1
446	064.52	3839.64	90.0	5.1
448	153.77	4023.36	90.0	5.1
449	182.88	4128.56	90.0	5.1
450	210.38	4048.54	90.0	5.1
451	179.45	3970.85	90.0	5.1
452	146.52	3889.81	90.0	5.1
453	99.79	3820.34	90.0	5.1
454	037.75	3751.18	90.0	5.1
456	037.99	3689.19	90.0	5.1
457	121.90	3785.62	90.0	5.1
458	186.09	3883.49	90.0	5.1
459	234.50	4006.49	90.0	5.1
460	264.92	4128.69	90.0	5.1
461	079.28	3672.85	90.0	5.1
462	159.97	3763.25	90.0	5.1
463	221.69	3867.47	90.0	5.1
464	273.65	3994.32	90.0	5.1
465	324.98	4005.30	90.0	5.1
466	395.53	3924.46	90.0	5.1
467	57.07	3846.60	90.0	5.1
468	118.14	3770.87	90.0	5.1
469	172.68	3704.85	90.0	5.1
470	122.00	3646.77	90.0	5.1
471	097.64	3628.62	90.0	5.1
472	089.39	3573.64	90.0	5.1
473	118.69	3586.14	90.0	5.1
474	210.37	3698.21	90.0	5.1
475	262.22	3765.90	90.0	5.1

RANGE-AZIMUTH ACCURACIES (CONTINUED)

<u>Fix No.</u>	<u>X Coordinate</u>	<u>Y Coordinate</u>	<u>Angle of Intersection</u>	<u>Radius of 90° Circle</u>
476	3317.64	3873.69	90.0	5.1
478	3336.64	3900.37	90.0	5.1
479	3335.51	3831.40	90.0	5.1
480	3303.12	3760.21	90.0	5.1
481	3258.28	3696.16	90.0	5.1
482	3212.24	3631.26	90.0	5.1
483	3165.13	3578.90	90.0	5.1
484	3129.45	3550.77	90.0	5.1
485	3142.92	3499.37	90.0	5.1
486	3214.10	3575.56	90.0	5.1
487	3280.84	3665.79	90.0	5.1
488	3344.31	3753.54	90.0	5.1
489	3395.65	3847.40	90.0	5.1
490	3420.41	3919.11	90.0	5.1
491	3466.94	3949.20	90.0	5.1
492	3399.67	3856.67	90.0	5.1
493	3395.38	3761.44	90.0	5.1
494	3355.71	3669.35	90.0	5.1
495	3275.38	3583.62	90.0	5.1
496	3197.78	3504.04	90.0	5.1
497	3161.00	3465.96	90.0	5.1

APPENDIX C

PROGRAM FOR 90 PERCENT CONFIDENCE ELLIPSE PARAMETERS

```
C PROGRAM NAME: ELLIP
C DESCRIPTION: COMPUTES ORIENTATION, 90% SIGMA-X, 90% SIGMA-Y,
C              FOR ERROR ELLIPSE ABOUT A HYDROGRAPHIC
C              POSITION ESTABLISHED BY RANGE-RANGE, AZIMUTH-
C              AZIMUTH OR RANGE-AZIMUTH POSITION
C
C AUTHCR: NICHOLAS E. PERUGINI
C        LT. NOAA
C        NAVAL POSTGRADUATE SCHOOL
C DATE:  SEPTEMBER , 1984
C
C      IMPLICIT REAL * 4 (A-H,C-Z)
C
C      INITIALIZE VALUES:  FOR RANGE-RANGE AND AZIMUTH-AZIMUTH:
C                          -XL AND YL ARE COORDINATES OF LEFT STATION
C                          -XR AND YR ARE COORDINATES OF RIGHT STATION
C                          -SIGL AND SIGR ARE RESPECTIVE STANDARD ERRORS
C                          ASSOCIATED WITH EACH LOP
C
C                          FOR RANGE-AZIMUTH:
C                          -XL AND YL ARE COORDINATES OF OCCUPIED STATION
C                          -SIGL IS SIGMA OF THEODOLITE LOP
C                          -SIGR IS SIGMA OF RANGE LOP
C *****
C      XL=4914.75
C      YL=2009.86
C      SIGL=3.0
C
C      XR=2474.75
C      YR=4247.42
C      SIGR= 3.0
C
C      ENTER CORRELATION COEFFICIENT:  USUALLY ZERO FOR R-R,
C      R-AZ, AND AZ-AZ
C      RC = 0.0
C      PI=3.141593
C
C      ENTER INDICATOR TO TELL WHAT KIND OF DATA IS ENTERING PROGRAM
C      IND = 1  RANGE-RANGE
C      IND = 2  AZIMUTH-AZIMUTH
C      IND = 3  RANGE-AZIMUTH
C *****
C      IND=1
C *****
C      INC IS A TOGGLE WHICH CHECKS FOR BETA GREATER THAN 90 DEG.
C      NOTHING IN PROGRAM SHOULD BE CHANGED FROM HERE ON
C
C      READ IN DATA FROM DATA FILE:  IFIX = FIX NUMBER
C      EX  = X COORDINATE OF HYDRO POSITION
C      EY  = Y COORDINATE OF HYDRO POSITION
C      ID  = ANGLE OF INTERSECTION IN DEGREES
C      SENTINEL IS IFIX = 999, TELLS PROGRAM TO STOP READING
C
C      10  CCNTINUE
```



```

20 READ(4,20) IFIX,ILL,PX,EY,TD,RAD
FCRMT(1X,I3,3X,I1,5X,F7.2,6X,F7.2,5X,F8.4,3X,F5.2)
INC = 0
IF(IFIX.EQ.999) GO TO 900
IF(TD.LT.90.) LD=TD
IF(TD.LT.90.) GO TO 30
C WORK WITH BETA LESS THAN 90 DEGREES: TOGGLE TURNED ON TO ONE
DE=180.-TD
INC=1
30 CCNTINUE
C
C KEEP TANGENT FUNCTION FROM BEING UNDEFINED IN A RARE CASE
C OF THE FIX AND CONTROL STATION HAVING SAME COORDINATES
IF(FX.EQ.XL) FX=PX+ 0.5
IF(FY.EQ.YL) FY=PY+ 0.5
C
C CHANGE DEGREES TO RADIANS
BETA=.01745329*DD
C USE LEFT STATION AS BASIS FOR COMPUTATIONS
C ORIENTATION ANGLES WILL BE FIXED WITH RESPECT TO LEFT LOP
C
C FINE AZIMUTH FROM NORTH BETWEEN HYDRO POSITION AND LEFT
C STATION. AZIMUTH WILL BE DEFINED BETWEEN 0-180 DEGREES
C MEASURED CLOCKWISE FROM NORTH.
C THIS IS THE RANGE-RANGE AZIMUTH DETERMINATION.
IF(IND.EQ.1) GO TO 40
IF(PY.GE.YL) THEN
  IF(PX.GE.XL) THEN
    ALPHA = PI-ATAN((PY-YL)/(PX-XL))
  ELSE
    ALPHA = ATAN((PY-YL)/(XL-PX))
  END IF
ELSE
  IF(PX.GE.XL) THEN
    ALPHA = ATAN((YL-PY)/(PX-XL))
  ELSE
    ALPHA = PI-ATAN((YL-PY)/(XL-PX))
  END IF
END IF
GC TO 60
C AZIMUTH FIXING FOR AZIMUTH-AZIMUTH POSITIONS
40 CCNTINUE
C
C
IF(FY.GE.YL) THEN
  IF(PX.GE.XL) THEN
    ALPHA = ATAN((PX-XL)/(PY-YL))
  ELSE
    ALPHA = PI-ATAN((XL-PX)/(PY-YL))
  END IF
ELSE
  IF(PX.GE.XL) THEN
    ALPHA = PI-ATAN((PX-XL)/(YL-PY))
  ELSE
    ALPHA = ATAN((XL-PX)/(YL-PY))
  END IF
END IF
C
C AZIMUTH EQUALS THETA FOR RANGE AZIMUTH CASE, ASSUMING
C THEODOLITE SIGMA IS LESS THAN RANGE SIGMA
C
IF(IND.EQ.3) GC TO 70
C
C BEGIN COMPUTING THETA, THAT IS THE ANGLE OF ROTATION FROM
C LEFT LCP
60 CCNTINUE
B1=SIGL**2*SIN(2*BETA)+2*RO*SIGL*SIGR*SIN(BETA)

```

```

      B2=SIGL**2*COS(2*BETA)+2*RO*SIGL*SIGR*COS(BETA)+SIGR**2
      IF (ABS(B2).LT.0.0001) E2=.0001
      E3=E1/B2
C COMPUTE ROTATION ANGLE FROM LEFT LOP
      TH=0.5*ATAN(B3)
      90 CCNTINUE
C
C DEFINE SEMI-MAJOR AXES ORIENTATION IN TERMS OF 0-180 DEGREES
C ROTATION, CLOCKWISE FROM NORTH
C
C RANGE-RANGE CASE
      IF (IND.EQ.1) THEN
        IF (INC.EQ.1) THETA=ALPHA+TH
        IF (INC.EQ.0) THETA=ALPHA-TH
      END IF
C
C AZIMUTH-AZIMUTH CASE
      IF (IND.EQ.2) THEN
        IF (INC.EQ.0) THETA=ALPHA+TH
        IF (INC.EQ.1) THETA=ALPHA-TH
      END IF
C
C FIX ROTATION ANGLE FROM 0-180 DEGREES
      70 CCNTINUE
C CONDITION FOR RANGE-AZIMUTH DATA
      IF (IND.EQ.3) THETA=ALPHA
      IF (THETA.LT.0.) THETA=PI+THETA
      IF (THETA.GT.PI) THETA=THETA-PI
C DEG IS THE SEMI-MAJOR ELLIPSE AXIS ORIENTATION IN DEGREES
      DEG=57.295779*THETA
C COMPUTE 90% SIGMAX AND SIGMAY OF ERROR ELLIPSE
      CALL PROB(SIGL,SIGR,RO,TD,SGX90,SGY90,RADIUS,ELAF,CIRAR)
      WRITE(7,100) IFIX,IX,PI,TD,SGX90,SGY90,DEG
      100 FCORMAT(IX,I3,3X,F7.2,3X,F7.2,3X,F5.1,3X,F4.1,3X,F4.1,
        * 3X,F5.1)
      GC TO 10
      900 CCNTINUE
      STOP
      END

```

APPENDIX D

ACCURACY CLASSIFICATION: 90 PERCENT CONFIDENCE ELLIPSES

CLASSIFIED RANGE-RANGE POSITIONS

Control Stations: BEACH LAB 1982 and MUSSEL 1932

Standard Error Used in Computations: 3 meters

Fix No.	X Coord.	Y Coord.	Beta	90% Sigma X	90% Sigma Y	Orientation
1	2668.05	4942.07	127.0	10.2	5.1	79.0
2	2852.01	5076.69	121.6	9.3	5.2	85.3
3	3041.58	5194.85	118.6	8.9	5.3	90.2
4	3040.27	5148.74	117.0	8.7	5.3	90.6
5	2838.26	5021.35	120.3	9.1	5.2	85.3
6	2640.06	4877.13	126.9	10.2	5.1	78.1
7	2553.46	4752.36	130.4	10.9	5.0	74.1
8	2724.10	4885.47	121.4	9.3	5.2	82.0
9	2889.06	5013.63	117.6	8.8	5.3	87.2
10	2975.61	5124.37	115.0	8.5	5.4	91.9
11	3172.63	5136.23	112.7	8.2	5.5	94.5
12	2958.13	5006.65	114.4	8.4	5.4	89.7
13	2771.33	4876.02	118.0	8.8	5.3	84.2
14	2681.02	4729.89	127.0	10.2	5.1	75.9
15	2884.41	4665.31	124.0	9.7	5.2	76.7
16	2740.05	4805.63	116.7	8.7	5.3	83.8
17	2913.27	4928.51	112.8	8.2	5.5	89.2
18	3097.44	5047.77	111.2	8.1	5.5	93.5
19	3193.94	5103.46	110.9	8.0	5.5	95.5
20	2672.47	4659.05	118.8	8.9	5.4	79.8
21	2762.15	4769.60	113.2	8.3	5.5	81.4
22	2904.91	4875.24	110.5	8.0	5.5	89.7
23	3056.38	4975.73	109.3	7.9	5.6	93.3
24	3133.36	5064.00	108.9	7.8	5.6	96.3
25	3133.36	5101.96	107.1	7.7	5.7	100.0
26	3115.64	5007.38	106.8	7.6	5.7	96.7
27	3015.45	4900.75	107.1	7.7	5.7	93.2
28	2839.38	4778.31	108.7	7.8	5.6	88.9
29	2679.99	4651.31	112.8	8.2	5.5	83.4
30	2727.88	4632.77	106.9	7.6	5.7	86.7
31	2899.83	4776.97	105.2	7.5	5.7	91.3
32	3099.77	4901.75	104.4	7.4	5.8	95.6
33	3255.42	5019.92	105.0	7.5	5.7	99.2
34	3372.07	5123.36	106.0	7.6	5.7	102.6
35	3479.02	5151.09	105.3	7.5	5.7	106.2
36	3474.77	5065.57	104.1	7.4	5.8	102.7
37	3257.48	4953.37	102.7	7.3	5.8	99.3
38	3043.03	4821.88	101.7	7.2	5.9	95.5
39	2845.07	4680.80	101.7	7.2	5.9	91.4
40	2746.96	4608.32	103.1	7.3	5.8	88.6

CLASSIFIED AZIMUTH-AZIMUTH POSITIONS

Control Stations: USE MON 1978 and MUSSEL 1932

Standard Error Used in Computations: 1.3 meters

Fix No.	X Coord.	Y Coord.	Beta	90% Sigma X	90% Sigma Y	Orientation
619	4449.26	2711.40	156.9	9.8	2.0	139.4
620	4437.86	2807.29	153.0	8.5	2.0	139.8
621	4427.41	2897.17	149.6	7.5	2.0	139.8
622	4419.65	2989.36	146.2	6.8	2.1	139.8
623	4410.42	3072.20	143.4	6.3	2.1	139.6
624	4399.60	3154.04	141.3	5.9	2.1	139.6
625	4376.52	3234.24	138.9	5.6	2.1	138.6
626	4364.31	3319.82	136.2	5.3	2.1	138.0
627	4348.71	3411.24	133.5	5.0	2.1	137.5
628	4334.31	3502.51	130.7	4.7	2.2	136.5
631	4338.97	3381.55	135.1	5.2	2.1	137.4
632	4337.95	3290.68	138.7	5.6	2.1	137.8
633	4327.70	3199.92	142.8	6.2	2.1	138.2
634	4322.53	3107.83	146.9	6.9	2.1	138.8
635	4323.18	3012.49	151.0	7.9	2.0	139.8
636	4324.42	2916.00	155.3	9.2	2.0	138.8
637	4327.25	2818.39	159.8	11.3	2.0	137.7
638	4394.77	2806.86	156.0	9.5	2.0	138.9
639	4386.58	2903.09	152.0	8.2	2.0	139.1
640	4377.29	2998.63	148.4	7.2	2.1	139.9
641	4367.00	3090.26	145.1	6.6	2.1	138.9
642	4355.55	3187.06	141.9	6.0	2.1	138.5
643	4345.97	3288.88	138.5	5.6	2.1	138.0
644	4256.90	3516.02	133.6	5.0	2.1	135.5
645	4260.68	3416.65	137.4	5.4	2.1	136.2
646	4264.77	3321.01	141.1	5.9	2.1	136.6
647	4283.59	3208.82	144.8	6.5	2.1	137.5
648	4293.24	3127.36	147.7	7.1	2.1	137.8
649	4300.30	3024.70	151.8	8.1	2.0	137.9
650	4345.53	3145.58	144.1	6.4	2.1	138.5
651	4370.38	3236.09	139.1	5.7	2.1	138.5
652	4398.77	3327.77	134.2	5.1	2.1	138.4
653	4411.48	3421.46	130.2	4.7	2.2	138.0
654	4438.30	3506.23	125.9	4.3	2.2	137.7
655	4470.97	3591.21	121.6	4.0	2.3	137.4
656	4502.73	3677.50	117.4	3.8	2.3	137.0
657	4514.38	3767.26	114.0	3.6	2.4	136.2
658	4512.00	3860.13	111.1	3.5	2.4	135.2
659	4520.10	3948.53	107.9	3.4	2.4	134.3
660	4454.79	3049.75	139.2	5.7	2.1	141.0

CLASSIFIED RANGE-AZIMUTH POSITIONS

Control Stations: USE MON 1978, MUSSEL 1932

Standard Errors: RANGE--3 meters; T-2--1.3

Fix No.	X Coord.	Y Coord.	Beta	90% Sigma X	90% Sigma Y	Orientation
414	2898.58	4611.99	90.0	6.4	2.8	49
415	2979.40	4483.31	90.0	6.4	2.8	64.
416	3027.69	4342.47	90.0	6.4	2.8	80.
417	2795.26	4216.04	90.0	6.4	2.8	95.6
418	3002.90	4061.15	90.0	6.4	2.8	100.4
419	2933.58	3933.67	90.0	6.4	2.8	123.6
420	2904.53	3888.38	90.0	6.4	2.8	129.9
421	2955.47	3388.99	90.0	6.4	2.8	140.9
422	3128.22	3488.78	90.0	6.4	2.8	150.9
422	3048.17	3599.79	90.0	6.4	2.8	153.5
424	2991.68	3723.65	90.0	6.4	2.8	155.5
425	2911.61	3333.20	90.0	6.4	2.8	155.5
426	2833.62	3922.16	90.0	6.4	2.8	155.5
427	2749.17	4000.71	90.0	6.4	2.8	155.5
428	2755.46	4020.99	90.0	6.4	2.8	155.5
429	2822.93	3966.92	90.0	6.4	2.8	155.5
430	2854.60	3922.66	90.0	6.4	2.8	155.5
431	2907.95	3883.53	90.0	6.4	2.8	155.5
432	2961.44	3901.64	90.0	6.4	2.8	155.5
433	3005.23	3988.11	90.0	6.4	2.8	116.7
434	3037.78	4055.01	90.0	6.4	2.8	108.6
435	3065.09	4134.51	90.0	6.4	2.8	100.8
436	3074.88	4036.74	90.0	6.4	2.8	109.3
437	3048.02	3955.93	90.0	6.4	2.8	117.1
438	2999.76	3888.71	90.0	6.4	2.8	125.7
439	2943.19	3805.76	90.0	6.4	2.8	133.1
440	3098.59	4049.87	90.0	6.4	2.8	133.1
441	3098.84	3997.78	90.0	6.4	2.8	106.8
442	3058.84	3897.24	90.0	6.4	2.8	113.4
443	3009.61	3822.58	90.0	6.4	2.8	128.2
444	2914.71	3837.97	90.0	6.4	2.8	132.6
445	3008.50	3755.28	90.0	6.4	2.8	132.7
446	3064.52	3833.64	90.0	6.4	2.8	124.7
448	3153.77	4023.36	90.0	6.4	2.8	108.3
449	3182.88	4128.56	90.0	6.4	2.8	99.5
450	3210.38	4048.54	90.0	6.4	2.8	105.1
451	3179.45	3970.85	90.0	6.4	2.8	111.4
452	3146.52	3889.81	90.0	6.4	2.8	118.0
453	3099.79	3820.34	90.0	6.4	2.8	124.6
454	3047.75	3751.18	90.0	6.4	2.8	130.9

LIST OF REFERENCES

1. Kaplan, A., Error Analysis of Hydrographic Positioning and the Application of Least Squares, M. S. Thesis, Naval Postgraduate School, Monterey, 1980.
2. Heinzen, M. R., Hydrographic Surveys: Geodetic Control Criteria, M. S. Thesis, Cornell University, 1977.
3. Naval Warfare Research Center Research Memorandum NWRC-RM34, Stanford Research Institute, Menlo Park, CA., Mathematical Considerations Pertaining to the Accuracy of Position Location and Navigation Systems, Part I, by W. A. Burt and others, 1966.
4. Adams, K. I., Hydrographic Manual, U.S. Coast and Geodetic Survey, 1942.
5. International Hydrographic Organization Special Publication No. 44 (2nd Edition), International Hydrographic Organization Standards for Hydrographic Surveys and Classification Criteria for Deep Sea Soundings, 1982.
6. Wallace, J. L., telephone conversation, National Oceanic and Atmospheric Administration, National Ocean Service, Rockville, MD, June 1984.
7. Laurila, S. H., Electronic Surveying and Navigation, John Wiley & Sons, 1976.
8. Davis, R. E., and others, Surveying Theory and Practice, McGraw-Hill, 1981.
9. Munson, R. C., Positioning Systems: Report on the Work of WG414b, paper presented at the XV International Congress of Surveyors, Stockholm, Sweden, 1977.
10. Bowditch, N., American Practical Navigator, Defense Mapping Agency Hydrographic Center, 1977.
11. Hecover, W. E., Algorithms for Confidence Circles and Ellipses, unpublished paper, National Oceanic and Atmospheric Administration, Woods Hole, MA, June 1984.
12. ACIC Technical Report No. 96, USAF Aeronautical Chart and Information Center, St. Louis, MO, Principles of Error Theory and Cartographic Applications, by C. R. Greenwalt and M. E. Schultz, 1962.

13. Waltz, D. A., An Error Analysis of Range-Azimuth Positioning, M. S. Thesis, Naval Postgraduate School, Monterey, 1983.
14. Umlach, M. J., Hydrographic Manual Fourth Edition, National Oceanic and Atmospheric Administration, National Ocean Survey, 1976.
15. Harter, H. L., "Circular Error Probabilities," Journal of the American Statistical Association, Vol. 55, December 1960.
16. NPS Technical Note VM-12, Using DISSPLA at NPS, Naval Postgraduate School, Monterey, June 1984.
17. National Ocean Survey Technical Manual No. 1, HYDROPLOT/HYDRICLOG SYSTEM MANUAL, by J. L. Wallace, 1977.

INITIAL DISTRIBUTION LIST

	No.	Copies
1. Defense Technical Information Center Cameron Station Alexandria, VA 22314	2	
2. Library, Code 0142 Naval Postgraduate School Monterey, CA 93943	2	
3. Chairman, Department of Oceanography Code 68Mr Naval Postgraduate School Monterey, CA 93943	1	
4. NCAA Liaison Officer Post Office Box 8688 Monterey, CA 93943	1	
5. Professor Joseph J. von Schwind Code 68Vs Naval Postgraduate School Monterey, CA 93943	1	
6. Lt. Nicholas E. Ferugini NOAA Ship RAINIER 1801 Fairview Avenue, East Seattle, WA 98102	1	
7. Office of the Director Naval Oceanography Division (OP-952) Department of the Navy Washington, D.C. 20350	1	
8. Commander Naval Oceanography Command NSTL, MS 39529	1	
9. Commanding Officer Naval Oceanographic Office Bay St. Louis NSTL, MS 39522	1	
10. Commanding Officer Naval Ocean Research and Development Activity Bay St. Louis NSTL, MS 39522	1	

11. Chief of Naval Research 1
800 N. Quincy Street
Arlington, VA 22217
12. Chairman, Oceanography Department 1
U. S. Naval Academy
Annapolis, MD 21402
13. Chief, Hydrographic Programs Division 1
Defense Mapping Agency (Code PPH)
Building 56
U.S. Naval Observatory
Washington, D.C. 20305-3000
14. Associate Deputy Director for Hydrography 1
Defense Mapping Agency (Code DH)
Building 56
U.S. Naval Observatory
Washington, D.C. 20305-3000
15. Topographic Sciences Department 1
Code TSD-MC
Defense Mapping School
Ft. Belvoir, VA 22060-5828
16. Director Charting and Geodetic Services 1
N/CG, Room 1006, WSC-1
National Oceanic and Atmospheric Administration
Rockville, MD 20852
17. Chief, Nautical Charting Division 1
N/CG2, Room 1003, WSC-1
National Oceanic and Atmospheric Administration
Rockville, MD 20852
18. Chief, Hydrographic Surveys Branch 1
N/CG24, Room 404, WSC-1
National Oceanic and Atmospheric Administration
Rockville, MD 20852
19. Program Planning, Liaison, and Training Div. 1
NC2, Room 105, Rockwell Building
National Oceanic and Atmospheric Administration
Rockville, MD 20852
20. Director, Pacific Marine Center 1
N/MCP
National Ocean Service, NOAA
1801 Fairview Avenue, East
Seattle, WA 98102
21. Director, Atlantic Marine Center 1
N/MCA
National Ocean Service, NOAA
439 West York Street
Norfolk, VA 23510
22. Chief, Program Services Division 1
N/MCA2
National Ocean Service, NOAA
439 West York Street
Norfolk, VA 23510
23. Lt. Bruce Hillard, NOAA 1
NOAA Ship DAVIDSON
1801 Fairview Avenue, East
Seattle, WA 98102

- 24. Mr. Mark Faye
430 Cedar Lane
East Meadow, NY 11554
- 25. Mr. John Kolesar
278 Tripp St.
Swoyersville, PA 18704
- 26. Mr. Edward N. Perugini
72 Maltby Ave.
Swoyersville, PA 18704

1

1

2

